Journal of Human Evolution 189 (2024) 103512

Contents lists available at ScienceDirect

Journal of Human Evolution

journal homepage: www.elsevier.com/locate/jhevol

JHumEvo

Finite element analysis of Neanderthal and early *Homo sapiens* maxillary central incisor

Ali Najafzadeh [a,b,1], María Hernaiz-García [a,1], Stefano Benazzi [c], Bernard Chen [d], Jean-Jacques Hublin [e,f], Ottmar Kullmer [g,h], Ariel Pokhojaev [i], Rachel Sarig [i,j], Rita Sorrentino [c,k], Antonino Vazzana [c], Luca Fiorenza [a,*]

[a] Monash Biomedicine Discovery Institute, Department of Anatomy and Developmental Biology, Monash University, Melbourne, VIC, 3800, Australia
[b] Department of Mechanical and Aerospace Engineering, Monash University, Melbourne, VIC, 3800, Australia
[c] Department of Cultural Heritage, University of Bologna, Ravenna, 48121, Italy
[d] Department of Surgery, The University of Melbourne, Melbourne, VIC, 3010, Australia
[e] Chaire de Paléoanthropologie, CIRB (UMR 7241-U1050), Collège de France, 11, Place Marcelin-Berthelot, 75231, Paris, Cedex 05, France
[f] Max Planck Institute for Evolutionary Anthropology, Leipzig, 04103, Germany
[g] Division of Palaeoanthropology, Senckenberg Research Institute and Natural History Museum Frankfurt, Frankfurt a. M, 60325, Germany
[h] Department of Palaeobiology and Environment, Institute of Ecology, Evolution, and Diversity, Goethe University, Frankfurt a. M, 60438, Germany
[i] Department of Oral Biology, The Goldschleger School of Dental Medicine, Sackler Faculty of Medicine, Tel Aviv University, Tel Aviv, 69978, Israel
[j] Dan David Center for Human Evolution and Biohistory Research, Sackler Faculty of Medicine, Tel Aviv University, Tel Aviv, 69978, Israel
[k] Department of Biological, Geological and Environmental Sciences, University of Bologna, Bologna, 40126, Italy

ARTICLE INFO

Keywords:
Dental biomechanics
Anterior dental loading hypothesis
Bite force
Occlusal fingerprint analysis

ABSTRACT

Neanderthal anterior teeth are very large and have a distinctive morphology characterized by robust 'shovel-shaped' crowns. These features are frequently seen as adaptive responses in dissipating heavy mechanical loads resulting from masticatory and non-masticatory activities. Although the long-standing debate surrounding this hypothesis has played a central role in paleoanthropology, is still unclear if Neanderthal anterior teeth can resist high mechanical loads or not. A novel way to answer this question is to use a multidisciplinary approach that considers together tooth architecture, dental wear and jaw movements. The aim of this study is to functionally reposition the teeth of Le Moustier 1 (a Neanderthal adolescent) and Qafzeh 9 (an early *Homo sapiens* adolescent) derived from wear facet mapping, occlusal fingerprint analysis and physical dental restoration methods. The restored dental arches are then used to perform finite element analysis on the left central maxillary incisor during edge-to-edge occlusion. The results show stress distribution differences between Le Moustier 1 and Qafzeh 9, with the former displaying higher tensile stress in enamel around the lingual fossa but lower concentration of stress in the lingual aspect of the root surface. These results seem to suggest that the presence of labial convexity, lingual tubercle and of a large root surface in Le Moustier 1 incisor helps in dissipating mechanical stress. The absence of these dental features in Qafzeh 9 is compensated by the presence of a thicker enamel, which helps in reducing the stress in the tooth crown.

1. Introduction

One of the most distinct features of Neanderthal's dentition is certainly the presence of proportionally large anterior teeth compared to the molar crowns, usually not observed in other human groups (Molnar, 1972; Trinkaus, 1992). More specifically, the incisors display a morphology marked by a high degree of labial convexity, and by the presence of lingual marginal ridges (or shoveling) and well-developed lingual tubercles (Fig. 1; Bailey, 2006). It is however still not clear if the occurrence of these features is associated to adaptations related to feeding behavior (Wallace, 1975; Puech, 1981), genetic drift (Kimura et al., 2009; Hlusko et al., 2018), or to non-masticatory adaptations (Brace, 1964 Trinkaus, 1983; Le Cabec et al., 2013). In particular, several studies have argued that the high frequency and great expression

* Corresponding author.
E-mail address: luca.fiorenza@monash.edu (L. Fiorenza).
[1] The first two authors contributed equally to this work.

https://doi.org/10.1016/j.jhevol.2024.103512
Received 9 January 2023; Received in revised form 12 February 2024; Accepted 13 February 2024
Available online 10 March 2024
0047-2484/© 2024 The Authors. Published by Elsevier Ltd. This is an open access article under the CC BY license (http://creativecommons.org/licenses/by/4.0/).

of these dental traits in Neanderthals may represent an adaptive response for dissipating heavy mechanical loads resulting from masticatory and non-masticatory activities (Rak, 1986; Demes, 1987; Trinkaus, 1987; Smith and Paquette, 1989; Spencer and Demes, 1993).

This assumption—known as the anterior dental loading hypothesis (ADLH)—is based on the heavily worn front teeth found in most adult Neanderthal individuals (Brace, 1967; Wallace, 1975; Trinkaus, 1983; Rak, 1986). Neanderthal incisors and canines exhibit heavier wear than their molars, which are, in contrast, relatively unworn (Molnar, 1972; Trinkaus, 1992; Ungar et al., 1997; Clement et al., 2012; Krueger and Ungar, 2012; Krueger et al., 2017; Fiorenza et al., 2019, 2020). The high frequency of enamel chipping, antemortem tooth loss and microfractures of the anterior teeth, have been considered as signals of extensive use of teeth as a third hand, in tearing, holding and shaping a variety of objects (Weaver, 2009; Fiorenza and Kullmer, 2013, 2015). According to the ADLH, Neanderthal cranio-dental morphology adapted to sustain high-magnitude loads caused by masticatory and para-masticatory activities (Rak, 1986; Demes, 1987; Trinkaus, 1987; Smith and Paquette, 1989; Spencer and Demes, 1993). However, some studies have shown that Neanderthals were actually not capable to produce greater bite forces compared to modern humans (Anton, 1994; O'Connor et al., 2005; Wroe et al., 2018).

The central arguments revolving around the ADLH focus on the unique and bulging tooth morphology of Neanderthals incisors and canines, and on the heavy wear of their anterior teeth. Specifically, it has been hypothesized that incisor shoveling, together with prominent lingual tubercles and large anterior roots, represent adaptations to decrease the amount of stress generated from heavy or frequent loads (Trinkaus, 1986; Le Cabec et al., 2013). The presence of significant larger roots and greater root surface areas than in modern human anterior teeth probably would have helped Neanderthals to better resist higher or repetitive mechanical loads on the anterior dentition (Le Cabec et al., 2013).

However, all studies that biomechanically evaluated whether Neanderthal morphology met the adaptive needs to better sustain high-magnitude forces resulting from both masticatory and para-masticatory activities, only focused on the analysis of the face and did not include the dentition. To date, there are no biomechanical studies that analyzed Neanderthal anterior teeth.

The major objective of our study is to investigate how mechanical stress is distributed in the maxillary central incisors by analyzing and comparing the dentition of the Neanderthal specimen of Le Moustier 1 with the early *Homo sapiens* specimen of Qafzeh 9. Le Moustier 1 was an adolescent male individual dated between 46 and 42 ka (Valladas et al., 1986; Mellars and Grün, 1991; Maureille and Turq, 2005), and characterized by a complete and well-preserved dentition (with the exception of the right maxillary central incisor, which is missing postmortem, while the third molars are tilted and erupting; Daumas et al., 2021). Le Moustier 1 cranium has been reconstructed several times since its discovery in 1908 (Hoffmann, 1997). Unfortunately, the repeated assembling and disassembling of the various skeletal fragments caused physical damages and loss of some of the original osseous material (Thompson and Illerhaus, 1998; Ponce de León and Zollikofer, 1999; Ponce de León, 2002). Ponce de León and Zollikofer (1999) and Thompson and Illerhaus (1998) carried out two independent virtual reconstructions of Le Moustier 1 skull, that differ in a number of important details showing that subjectivity can lead to different results when dealing with computer-assisted methods (Bailey, 2007).

The Qafzeh sample consists of several specimens, recovered in a cave on the Mount of Precipitation located near Nazareth in the Lower Galilee, which were dated to ca. 115–94 ka (Schwarcz et al., 1988; Valladas et al., 1988). Qafzeh 9 is one of the most well preserved specimens with a complete dentition, probably belonging to a late adolescent/young adult female (Bruzek and Vandermeersch, 1997; Coqueugniot et al., 2000; Sarig et al., 2013a). However, the mandible and cranium of Qafzeh 9 are distorted, possibly due to taphonomic processes (Vandermeersch, 1981; Sarig et al., 2013a; Nogueira et al., 2019).

Consequently, the first aim of our study is to virtually restore the dental arches of Le Moustier 1 and Qafzeh 9 following a well-established method called occlusal fingerprint analysis (OFA; Kullmer et al., 2009), which is derived from wear facet mapping, and dental technical approaches for a reconstruction of the occlusal contacts of complementary wear facet pairs. The advantage of this method compared to previous approaches is that it relies on a reconstruction of occlusal movements with the repositioning of the physical models of the antagonistic crown pairs through a dental articulator. Subsequently the occlusal kinematics is validated through a virtual simulation using digital models of the reconstructed dental arches (Kullmer et al., 2013). This approach has been already successfully employed to reconstruct fragmented and deformed fossil remains such as the dental arches of *Rudapithecus hungaricus*, an extinct great ape from Late Miocene (Kullmer et al., 2013), and the *Australopithecus africanus* specimen Sts 52 (Benazzi et al.,

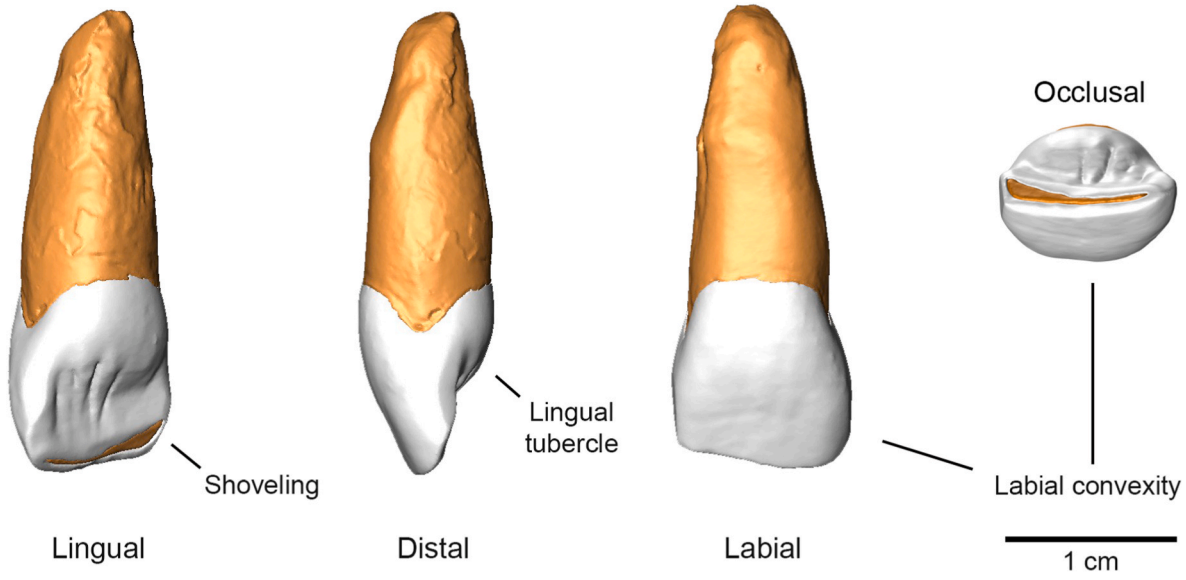

Fig. 1. Three-dimensional digital models of Le Moustier 1 maxillary left I^1 in lingual, distal, labial and occlusal views showing a moderate 'shovel-shaped' morphology with a well-developed lingual tubercle and a strong labial convexity.

2013a).

A correct alignment of the tooth crowns of Le Moustier 1 and Qafzeh 9 is essential for the examination of the mechanical behavior of incisor accessory dental traits by using an approach based on the kinematic study of the power stroke of the masticatory cycle and on finite element analysis (Benazzi et al., 2011a, 2015, 2016; Fiorenza et al., 2015). Finite element analysis is an engineering technique used to simulate stress, strain, and deformations in structures characterized by complicated geometries (Rayfield, 2007). The geometry of these structures is simplified by using a finite number of many smaller and simpler sub-regions, called elements, which are interconnected at nodal points, or nodes (Rayfield, 2007). For each element we assign structural and material properties which will define the way the finite element model will deform under specific applied loads and constraints (Panagiotopoulou, 2009).

In this study we will test if the presence of a strong lingual tubercle, well-developed labial curvature and large anterior root in Le Moustier 1 maxillary central incisors helps in dissipating the mechanical loads during edge-to-edge occlusion (where maxillary and mandibular anterior teeth meet along their incisal edges). This type of occlusion, which is the byproduct of heavy occlusal wear on the anterior teeth and lingual tipping of the incisors (Kaifu et al., 2003), was probably used for para-masticatory activities for cutting, holding and shaping a variety of objects (Brace, 1967; Molnar, 1972; Trinkaus, 1992; Fiorenza et al., 2019). We will compare Le Moustier 1 finite element results with those of Qafzeh 9, where these dental features are weakly expressed or absent. Moreover, because Neanderthal teeth are characterized by a relatively thinner enamel than in modern humans (Olejniczak et al., 2008; Smith et al., 2012), we will also evaluate how the mechanical stress is distributed in Le Moustier 1 and Qafzeh 9 maxillary incisor in relation to their enamel thickness.

2. Materials and methods

2.1. Materials

Le Moustier 1 represents the most completely preserved adolescent Neanderthal skeleton recovered to date. This fossil had a turbulent history: discovered in 1908 in France, it was later sold to the Museum für Völkerkunde in Berlin in 1910, where it was on display until 1945. At the end of World War II, the museum was destroyed by a bombing attack, and many of its remains lost forever (Hoffmann, 1997). Only years after, fragmented postcranial remains were recovered from the ruins of the museum. The cranial remains disappeared in the former Soviet Union but were later returned (1965) to the Museum für Vor-und Frühgeschichte in Berlin (Ponce de León and Zollikofer, 1999), where they are still stored to this date. The cranial remains consist of nine separated pieces, while the mandible is composed of two parts (Supplementary Online Material [SOM] Fig. S1; Thompson and Illerhaus, 1998; Ponce de León and Zollikofer, 1999). Some of the original material have been partially lost and damaged by repeated assembling and reassembling of the cranial remains through five reconstructions that mostly occurred at the beginning of the twentieth century (Klaatsch and Hauser, 1908; Klaatsch, 1909; Schuchardt, 1912; Dieck, 1923; Weinert, 1925). The dentition is fully preserved, with the exception of the right central maxillary incisor, which is missing. The second permanent molars are fully erupted and in occlusion, while the third molars are located apical the alveolar plane and do not show any sign of wear (Ponce de León and Zollikofer, 1999). Interestingly, the permanent left mandibular canine is impacted by the presence of the deciduous canine which is still in functional position (Thompson and Illerhaus, 1998; Ponce de León and Zollikofer, 1999).

Qafzeh 9 is the most complete specimen recovered from the Qafzeh site, which consists of 27 individuals dated to ca. 115–94 ka (Schwarcz et al., 1998; Valladas et al., 1988; Vandermeersch and Bar-Yosef, 2019). The remains of Qafzeh 9 are housed at the Dan David Center for Human Evolution (Faculty of Medicine, Tel Aviv University) and they probably belong to a female individual with an age estimated to be between 16 and 21 years (Bruzek and Vandermeersch, 1997; Coqueugniot et al., 2000; Sarig et al., 2013a; Nogueira et al., 2019). This specimen is characterized by a full and particularly well-preserved dentition. However, the mandible and the cranium are partially fragmented and show a certain degree of distortion, most likely associated to post-mortem taphonomic factors and to inadequate reconstruction (Vandermeersch, 1981; Tillier et al., 2004; Nicholson and Harvati, 2006; Sarig et al., 2013a; Nogueira et al., 2019). As a result of this deformation, mandible and maxilla of Qafzeh 9 do not articulate well (Sarig et al., 2013a). Sarig et al. (2013a) restored the occlusion of Qafzeh 9 to its original shape using a cast setup to correct the areas that were erroneously reconstructed. Their restoration showed that Qafzeh 9 was affected by anterior cross-bite, caused by the malposition of the left maxillary lateral incisor (Sarig et al., 2013a), and that may have locked the mandible in a position that deviates from centric occlusion. Moreover, the apex of the root is broken and incomplete.

In this study we focused on the biomechanical analysis of the left central maxillary incisor, which occludes with the antagonist lower central and lateral left incisors. We employed the Arizona State University Dental Anthropology System (ASUDAS), a standardized system consisting of a series of rank-scale plaques used to assess dental morphological (or nonmetric) variation (Turner et al., 1991; Scott and Turner, 1997). Because the ASUDAS system was developed to assess dental variability in modern human populations, we also included modifications developed for scoring dental traits in fossil hominin species (Martinón-Torres et al., 2007, 2012).

Le Moustier left I^1 is characterized by a moderate shoveling (score 1), a marked lingual tubercle (score 3) and by a well-developed labial curvature (score 2; SOM Table S1). In Qafzeh 9 central maxillary incisor the labial curvature and shoveling are not expressed (score 0), while double shoveling and lingual tuberculum are weakly developed (score 1). Moreover, while Le Moustier 1 left I^1 is characterized by a large and relatively short anterior root, Qafzeh 9 left I^1 displays a smaller but longer anterior root. Both incisors are characterized by a moderate degree of wear with dentine lines of distinct thickness (wear stage 3; Smith, 1984). Because the post-canine teeth of Qafzeh 9 and Le Moustier 1 are characterized by a lower degree of wear compared to the anterior dentition (relative to the first molar), and because permanent maxillary central incisors erupt at an older age than first permanent molars (Hillson, 2003), we can assume that these two individuals were already performing para-masticatory activities with their incisors (Clement et al., 2012).

Microtomographic scanning of Le Moustier 1 was carried out with a BIR ACTIS high-resolution CT scanner at the Department of Human Evolution of the Max Planck Institute for Evolutionary Anthropology, using the following scan parameters: 130 kV, 100 μA, 0.25 mm brass, and 5000 views per rotation (Benazzi et al., 2015, Fig. 1). Volume data were reconstructed using isometric voxels of 30.6 μm for the maxilla. Microtomographic scans of Qafzeh 9 were obtained at the Core Facility for micro-computed tomography at University of Vienna with a custom built VISCOM X8060 (Germany) μCT scanner using the following scanner parameters: 40–160 kV, 300–400 μA, 1400–2000msec, diamond high performance transmission target, 0.75 mm copper filter, isometric voxel sizes between 9 and 44 μm (SOM Fig. S2).

The μCT image data were semiautomatically segmented using Avizo v. 9.2 software (Thermo Fisher Scientific, Waltham), and the 3D models of the dental tissues (i.e., enamel and dentine) were refined in Geomagic Design v. X (3D Systems Software, Rock Hill) to optimize the triangles and create fully closed surfaces (Lugli et al., 2022).

We also calculated the bidimensional average enamel thickness (2D AET) and relative enamel thickness (2D RET; Kono, 2000) of Le Moustier 1 and Qafzeh 9 left I^1 after estimating the missing part of the cusp following the method published by O'Hara and Guatelli-Steinberg (2022) and compared these values with those of other Neanderthals,

fossil *Homo sapiens* and recent *Homo sapiens* obtained from literature (Smith et al., 2012).

The 2D AET index is the enamel surface divided by the length of the enamel-dentine junction (EDJ) surface, while 2D RET is obtained dividing 2D AET by the square root of coronal dentine (including the coronal pulp) area (Martin, 1985; Benazzi et al., 2014a). Moreover, because enamel thickness in 2D does not accurately capture the full distribution of enamel of the tooth crown (Olejniczak et al., 2008; Buti et al., 2017), we also calculated the 3D average and relative enamel thickness indices (3D AET and 3D RET) following general indications provided by Olejniczak et al. (2008) for molars, and subsequent guidelines outlined by Benazzi et al. (2014a) for the anterior dentition.

2.2. Occlusal restoration

Ponce de León and Zollikofer (1999) virtually reconstructed the cranio-dental remains of Le Moustier 1 taking into account occlusal wear for precise dental arch restoration. These authors classified occlusal wear into three major categories (general wear of occlusal surfaces, faceted wear of dental cusps, and interstitial attrition) through a stereomicroscope, and used this information to establish original areas of contact between adjacent teeth, and for matching the wear patterns between antagonist teeth (Ponce de León and Zollikofer, 1999). Sarig et al. (2013a) evaluated the occlusion of Qafzeh 9 by using a setup made of casts, focusing on those areas of mandibular teeth that did not align well with the maxillary dentition due to previous reconstructions. The casts were separated along the contact points and re-aligned to achieve maximum intercuspation.

Although the computer-assisted reconstruction of Le Moustier 1 and the cast setup of Qafzeh 9 probably represent good approximations of the original occlusal relationships of these fossil specimens, they were never validated. It therefore remains unclear if these oral restorations reflect the original physiological occlusion of these specimens (Benazzi et al., 2013b; Kullmer et al., 2013).

Methods derived from detailed wear facet mapping and dental-manual restorations have been recently employed for reconstructing the dental arches of important hominoid fossil specimens (Benazzi et al., 2013b; Kullmer et al., 2013). Previous reconstructions of hominin fossil specimens have been mainly based on qualitative observations and static occlusal positions. This, however, is not sufficient for a reliable functional dental arch restoration, since in a dynamic occlusal situation wear facets of the antagonist teeth move into contact sequentially depending on the trajectories of phase I and phase II occlusal power stroke motions (Kullmer et al., 2009, 2012). The advantage of the OFA approach is that a repositioning of each tooth crown (based on individual macrowear facet patterns) can be validated by applying

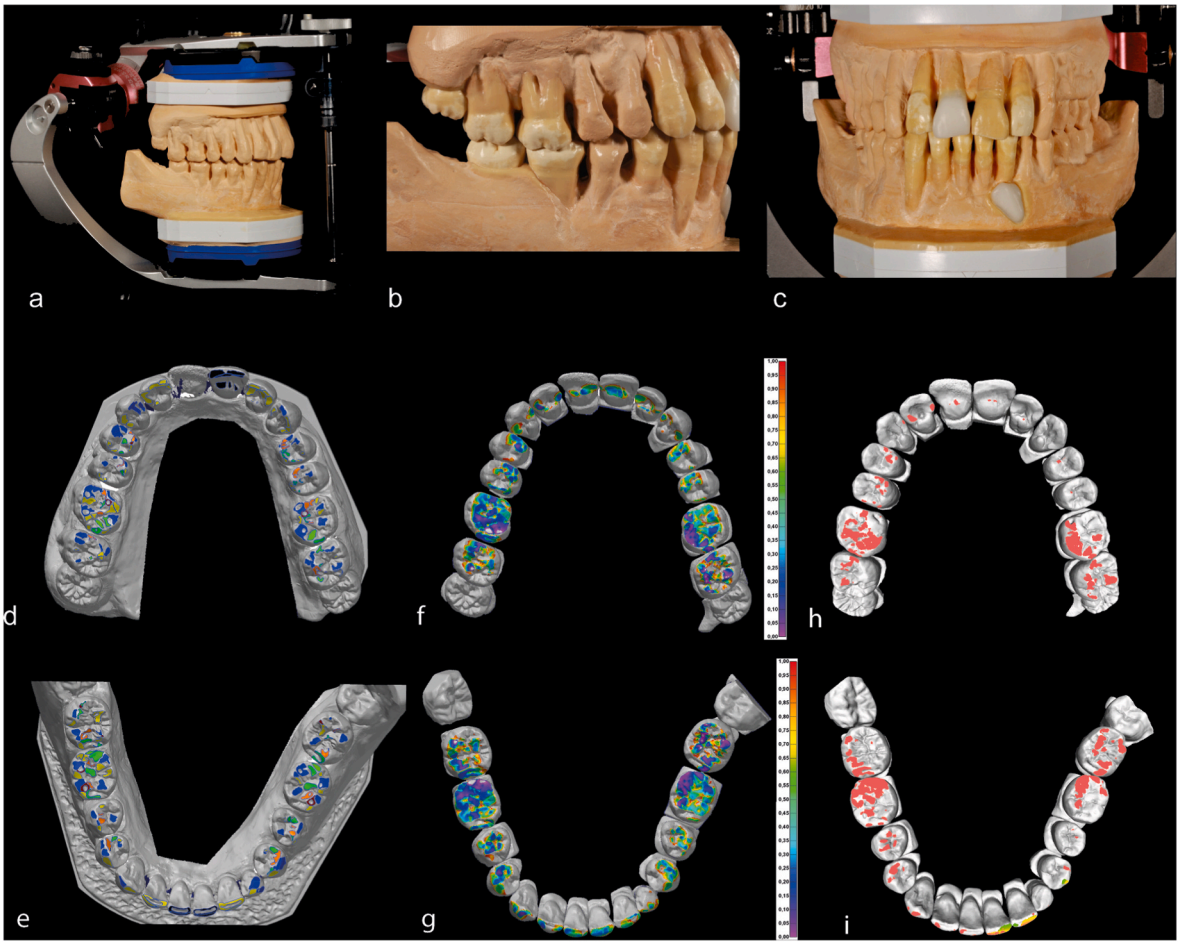

Fig. 2. Dental casts of Le Moustier 1 mounted in a dental articulator (PROTAR, KaVo; a). Lateral view of the right tooth row with repositioned crowns in maximum intercuspation (b). Frontal view of dental arch reconstruction in maximum intercuspation, showing an impacted lower canine and a replaced right I^1 (copied and mirrored left first I^1) in dental enamel color (c). Color-coded wear facet maps of the reconstructed dental arches following the concept of the occlusal fingerprint analysis (Kullmer et al., 2009; d and e). Color maps showing the deviation in maximum intercuspation occlusion (f and g). Purple and blue colors reflect full occlusal contacts at the locations wear facets. Occlusal contact maps obtained through the occlusal fingerprint analyzer software collision detection matching with the static occlusion of the physical reconstruction (h and i). (For interpretation of the references to color in this figure legend, the reader is referred to the Web version of this article.)

kinematic simulations; initially using a dental articulator with physical dental models, and then with digital models in the occlusal fingerprint analyzer v. 5.12.3 (Benazzi et al., 2011a) software, which allows the quantification of antagonistic sequential occlusal collisions between the 3D models (Kullmer et al., 2012, 2020). Thus, a tooth that is slightly deviating from its original position will produce occlusal interferences during the simulation, and it can be immediately identified as being incorrectly positioned.

We used high-resolution dental stone casts for each Le Moustier 1 and Qafzeh 9 tooth crown, and manually placed the dentition in a dental articulator (PROTAR, KaVo; Fig. 2a–c), which is designed to reproduce occlusion motions (Kullmer et al., 2012). The functional positions of the tooth crowns were realigned using the dental occlusal compass by attributing each antagonistic wear facet pair to its direction of movement (Kullmer et al., 2009). The restored dental arches were then surface scanned (smartSCAN 3D, Breuckmann GmbH; ca. 55 μm in average) and all wear facets were mapped manually on the virtual models (Fig. 2d and e; SOM Figs. S3a and d). The distance between the occlusal surfaces of antagonist teeth in maximum intercuspation was measured using a surface deviation analysis (Kullmer et al., 2013, Fig. 2f and g; SOM Figs. S3b and e). Finally, for the final test of a functional occlusion, the 3D models were loaded in the OFA software for the kinematic simulation of the occlusal contacts (Benazzi et al., 2013a; Kullmer et al., 2013, Fig. 2h and i; SOM Figs. S3c and f).

2.3. Kinematic simulation through the occlusal fingerprint analyzer software

The chewing cycle is a rhythmic process consisting of three phases that involves both opening and closing movements of the mandible (Kay and Hiiemae, 1974). The power stroke is particularly important because it is where the occlusal surfaces of the lower teeth shear over those of their maxillary counterparts, and where the effects of mastication in reducing the food bolus size in smaller pieces mostly occur (Kullmer et al., 2009). The OFA software is a virtual tool that can be used to test and analyze dental occlusal contacts during the power stroke movements of digital dental models, derived from collision detection algorithms (Kullmer et al., 2020). In an attempt to simulate an occlusal situation as realistic as possible we created digital split models with single crown models for the upper and lower dental rows. This allowed us to load the isolated crown models of the upper and lower dentition separately into two trajectory groups for the contact analyses. With such advanced trajectory groups, it is possible within the OFA software to simulate the periodontal shock absorption during antagonistic contacts, while it allows a slight and temporary displacement of maximum 50 μm of each crown during a contact situation.

By setting up a general pathway of motion for the lower dental arch crown models and a user-defined collision distance, we could simulate an incisor edge-to-edge bite of the repositioned dental arches of Le Moustier 1 and Qafzeh 9 (Fig. 3). We intended to simulate a retrusive movement of the lower jaw with a guidance of the crown relief along the incisor wear facets. Therefore, we started with a vice-versa movement of a protrusion of the lower jaw from the point of maximum intercuspation in order to use a defined contact situation as a start point. Subsequently we turned the motion of the pathway around, creating a trajectory developed through relief guidance of the incisors simulating an edge-to-edge bite situation. This is also called edge-to-edge protrusion (Cartagena et al., 1996). The mandible moves upward and retrusive along the surfaces of the incisors until the postcanine dentition takes over the guidance towards ending in maximum intercuspation. Finally, we used the detected contact areas of a sequential timestep of clear edge-to-edge contacts and calculated the resultant vector from the vertical and retrusive movements for the loading scenario in following finite element analyses (FEA).

2.4. Finite element analysis

Finite element analysis is a numerical technique that divides a structure into a finite number of discrete elements connected by points, or ‘nodes’. This interconnected network of elements and nodes constitutes the finite element volume mesh. We can then assign material properties that influence how the structure will react to predetermined loading conditions (Rayfield, 2007). With advances in computer software and imaging technology, FEA has reached a level of sophistication and accessibility that makes it a powerful tool in the testing of biomechanical hypotheses in studies of vertebrate form and function (Wroe et al., 2010). Increasingly, it has been applied to the study of feeding mechanics and dietary adaptations in humans and their relatives (Wroe et al., 2010, 2018; Strait et al., 2013; Ledogar et al., 2016).

The dental tissues (enamel, dentine and pulp) of the left central maxillary incisor were segmented in Avizo v. 9.2 and volumetric model of the specimen was reconstructed using isometric voxels of 30.6 μm for the maxilla following established protocols (Benazzi et al., 2014b). The periodontal ligament (PDL) was virtually created by offsetting the space around the root surface of 0.2 mm, which is an average value of those found in the literature (Hohmann et al., 2011; Xia et al., 2013; Benazzi et al., 2015). Finally, because recent studies have shown that the EDJ playing an important role in absorbing mechanical stress (Zaytsev and Panfilov, 2014), we modelled the EDJ as a layer of 0.1 mm between the enamel and dentine (Marshall et al., 2001).

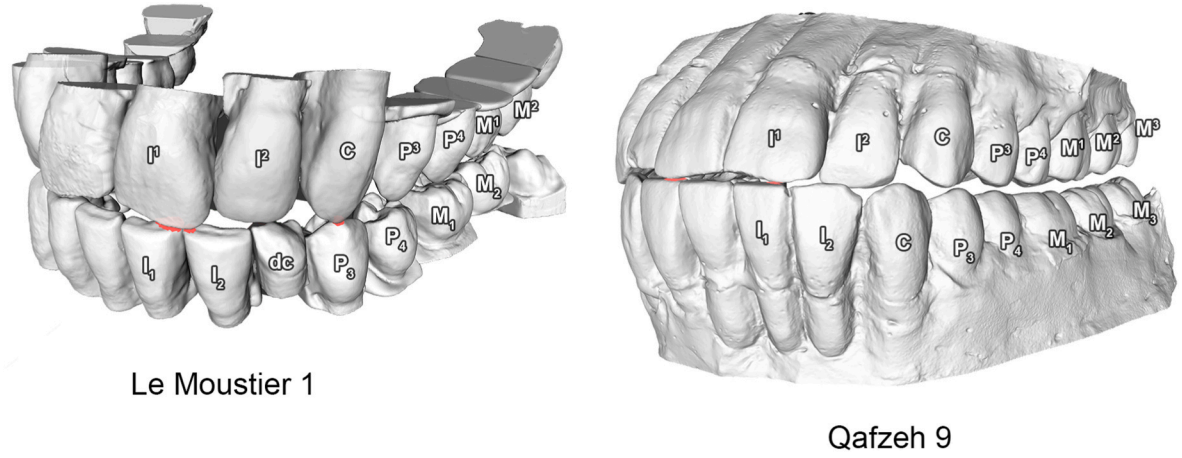

Fig. 3. Three-dimensional digital models of Le Moustier 1 and Qafzeh 9 upper and lower dental arches during edge-to-edge occlusion. In red color the occlusal contact areas between upper and lower teeth. (For interpretation of the references to color in this figure legend, the reader is referred to the Web version of this article.)

Smoothing and flattening were carried out in Geomagic Wrap v. 2021 (3D Systems, Rock Hill) as part of the FEA model preparation process as the analytical software is not able to cope with rough digital surfaces. As the supporting osseous tissues were not well-preserved in the original specimens (Ponce de León and Zollikofer, 1999; Thompson and Illerhaus, 2005; Sarig et al., 2013a), and because previous works on dental biomechanics showed that the dental supporting tissues (cortical and trabecular bone) do not interfere with the distribution of compressive and tensile stresses in the tooth (e.g., Benazzi et al., 2011a, 2013a, 2013c, 2014b, 2015, 2016), cortical and trabecular bone of Le Moustier 1 and Qafzeh 9 were virtually modelled in Geomagic Wrap v. 2021 (3D Systems, Rock Hill) using a cylindrical shape.

Thus, the whole reconstructed model consists of enamel, EDJ, dentine, pulp chamber, PDL, cortical and trabecular bone (Fig. 4). Assignment of material properties of tooth and bone tissues followed previously published protocols (SOM Table S2), and they were considered homogeneous, linearly elastic and isotropic, assumptions that are regularly applied with simpler continuum mechanics models (Fu et al., 2010). The tetrahedral meshes were created and optimized in Hyperworks v. 2019 (Altair Engineering Inc., Troy). The mesh was applied to the models with second order 10-noded elements (C3D10) to improve the precision of the stress calculation. Hence, the FEA mesh of Le Moustier 1 left I^1 consisted of 980,649 elements and 1,487,566 nodes, while the finite element mesh of Qafzeh 9 left I^1 contained 1,052,192 elements and 1,571,902 nodes.

The OFA software was used to virtually simulate the kinematics of Le Moustier 1 and Qafzeh 9 dentition and to obtain the trajectory of the upper incisor during an edge-to-edge bite (Fig. 5).

We selected the initial contact areas of the trajectory path since multiple sequential occlusal contacts are observable during the first bite and chewing motion. The OFA software was used to detect the loading areas for each of these two scenarios. The bite force of the Neanderthal molar (738.52 N) was used as the reference loading value, which was estimated based on skeletal data and jaw muscle architecture (Eng et al., 2013). For modern human anterior dentition, this force has been estimated to be 40% of that in the molar region (Bakke, 2006). As a result, a normal loading of 294.4 N was considered for the Le Moustier 1 edge-to-edge occlusion. Due to the different size of the incisors considered in this study, the load was scaled according to their occlusal surface. Mechanical stress (σ) is the measure of an external force acting over the cross-sectional area of an object (σ = force/area), and consequently an object with a larger area will be characterized by a lower stress if compared to a smaller object. To overcome this limitation, we applied the largest force in Le Moustier 1 (characterized by the largest incisor) and scaled down the force in Qafzeh 9 according to its smaller occlusal surface. In detail, because the occlusal surface of the Le Moustier 1 I^1 is the largest (13.41 mm^2), the load for Qafzeh 9 (occlusal surface = 8.60 mm^2) was scaled according to the ratio between its surface and Le Moustier 1's one, that is 188 N (scale factor = 0.64).

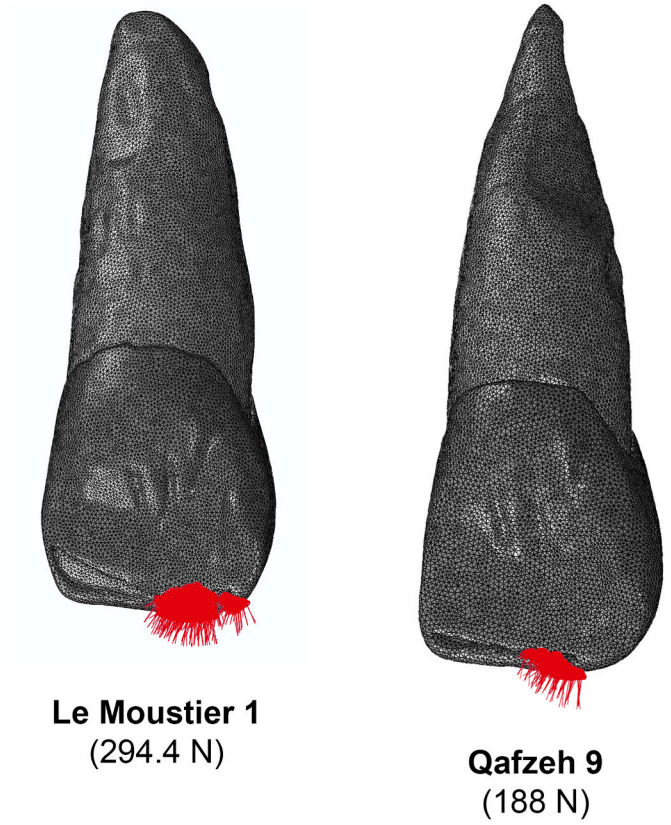

Fig. 5. Loading areas and directions during edge-to-edge bite in Le Moustier 1 (applied force = 294.4 N) and Qafzeh 9 (applied force = 188 N) left first maxillary incisors. The loading area (highlighted in red) was distributed proportionally according to the occlusal contact areas detected by the OFA software. The direction of the force (red arrows) was considered normal to the contact area. (For interpretation of the references to color in this figure legend, the reader is referred to the Web version of this article.)

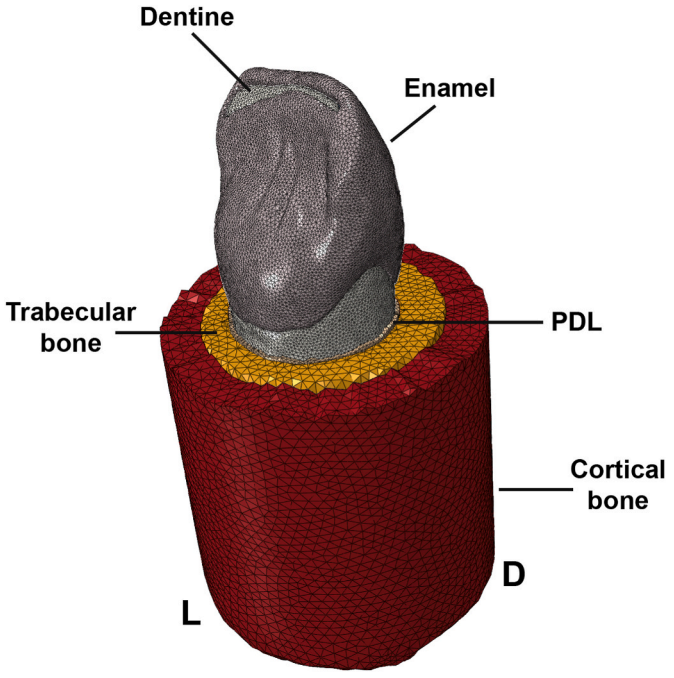

Fig. 4. Finite element mesh of Le Moustier 1 left central maxillary incisor showing the dental tissues and supporting structures: enamel, dentine, pulp chamber (not visible), periodontal ligament (PDL), cortical and trabecular bone. Abbreviations: L = lingual; D = distal.

The models and the loading areas were exported to Abaqus v. 2022 (Simulia, Vélizy-Villacoublay) for the FEA. The interfaces of the model were tied up to each other to ensure the proper conveyance of the stress values. The normal loads were applied perpendicularly to the surface elements of the loading areas. We virtually reconstructed the dental supporting tissues (cortical and trabecular bone) to create boundary conditions not directly fixed to the root.

For the FEA results we use color maps, which display areas of compressive and tensile stress of the 3D digital models. Traditionally, the color scheme used for FEA results of paleontological and biological specimens has been the classic 'rainbow' color map showing lower values in blue, higher values in red, and middle values in green and yellow (Wroe et al., 2010, 2018; Ledogar et al., 2016). However, despite their ubiquitous use, numerous studies have shown that 'rainbow' color maps can be problematic due to uneven color representation and its

inaccessibility for those with color vision deficiencies (Crameri et al., 2020; Lautenschlager, 2021). New tools are now available to create scientifically derived color maps to prevent data distortion and visual error (Harrower and Brewer, 2003; Van der Walt and Smith, 2015; Crameri, 2020). Here we used both 'rainbow' and 'inferno' color maps (Crameri, 2020), so that we can more accurately represent values of FEA models by showing higher discriminative power (Lautenschlager, 2021). The color map 'inferno' was imported in Abaqus v. 2022 (Simulia, Vélizy-Villacoublay) using a command-line script available in Lautenschlager (2021: Supplementary Material, Abaqus colors map).

3. Results

3.1. Enamel thickness

The 2D AET of Le Moustier 1 left I^1 is 0.65 mm, which is rather similar of 2D AET average values obtained from other Neanderthal central maxillary incisors (2D AET = 0.63) and recent *Homo sapiens* (2D AET = 0.62), but lower than those of fossil *Homo sapiens* (2D AET = 0.71; SOM Table S3). On the contrary, 2D AET of Qafzeh 9 left I^1 is 0.76, higher than average values for recent and fossil *Homo sapiens*. However, the 2D RET of Le Moustier 1 left I^1 is 7,29, significantly lower than

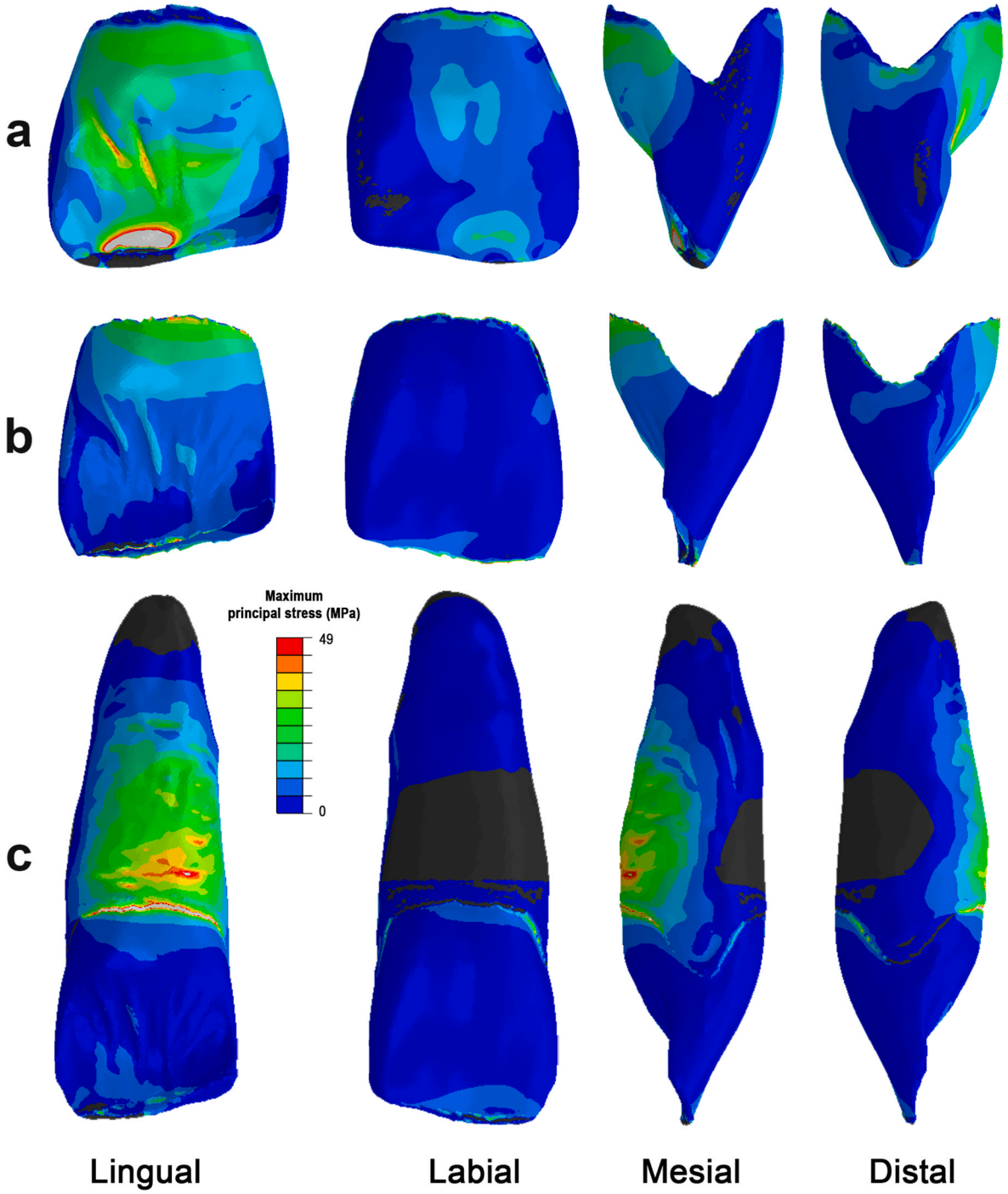

Fig. 6. Maximum principal stress distribution (MPa) of Le Moustier 1 left I^1 in lingual, labial, mesial and distal view during edge-to-edge occlusion (applied force = 294.4 N). Enamel (a), enamel-dentine junction (b) and dentine (c).

average values of other Neanderthals (2D RET = 9.19) and of those of fossil (2D RET = 10.57) and recent *Homo sapiens* (2D RET = 10.91; SOM Table S3). Qafzeh 9 left I^1 2D RET is 10.67, which is slightly lower than average values of fossil and recent *Homo sapiens*. Similar results are also found when we examine the 3D enamel thickness, with Le Moustier 1 left I^1 characterized by low 3D AET (0.65) and 3D RET (10.09) values, while Qafzeh 9 left I^1 displays significantly higher 3D AET (0.83) and 3D RET (12.37) values (SOM Table S3).

3.2. Finite element analysis results during edge-to-edge occlusion

During edge-to-edge occlusion the largest tensile stress in Le Moustier 1 left I^1 is located around the lingual fossa, and more specifically along the grooves lining the mesial marginal ridge, and towards the cervix (Fig. 6a, 7a and 8a; SOM Figs. S4a, S5g and S6a). Labially, we identify a few areas of moderate tensile stress; one near the labio-incisal edge, one in its central part, and one around the cervical line. Most of the tensile stress is absorbed at the EDJ level, especially around the cervix and along the incisal edge (Fig. 6b, 7b and 8a; SOM Figs. S4b, S5h and S6a), while the dentine of the crown shows no sign of tensile stress (Fig. 6c, 7c and 8a; SOM Figs. S4c, S5i and S6a). Interestingly, we found areas of moderate tensile stress around the mesial and distal aspects of the enamel tissue, just above the cervical line (Fig. 6a; SOM Fig. S4a). These areas of tensile stress tend to disappear at the EDJ.

In enamel, the compressive stress of Le Moustier 1 is mostly concentrated on the incisal edge, in correspondence of the occlusal contact with the opposite lower permanent incisor, and along the labial surface (SOM Figs. S5a, S5d, S7a, S8a, S9a and S10a). In particular, in the labial aspect of the crown we observe two areas with high compressive stress values, a larger one located just apical to the loaded region, and another smaller one which develops toward the cervix and it extends more distally. The EDJ absorbs most of the compressive stress, which is still visible along the incisal edge, both lingually and labially, and along the cervical line on the disto-labial aspect (SOM Figs. S5b, S5e, S7b, S8b, S9a and S10a). Smaller areas of compressive stress can also be observed in the crown dentine along the incisal contact with the lower incisor, and along the cervix in its labial and distal aspects (SOM Figs. S5c, S5f, S7c, S8c, S9a and S10a).

The tensile stress of Qafzeh 9 left I^1 is primarily distributed along the lingual cingulum and on its mesial and distal aspects (Figs. 7d, 8a and

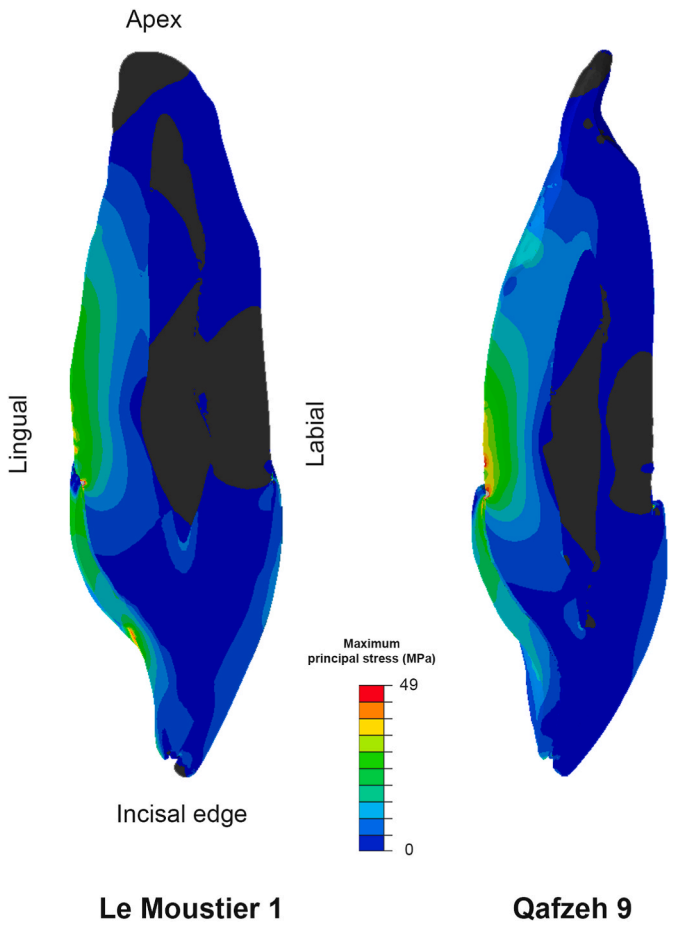

Fig. 8. Maximum principal stress distribution (MPa) of Le Moustier 1 (applied force = 294.4 N) and Qafzeh 9 (applied force = 188 N) left I^1 in midsagittal view during edge-to-edge occlusion.

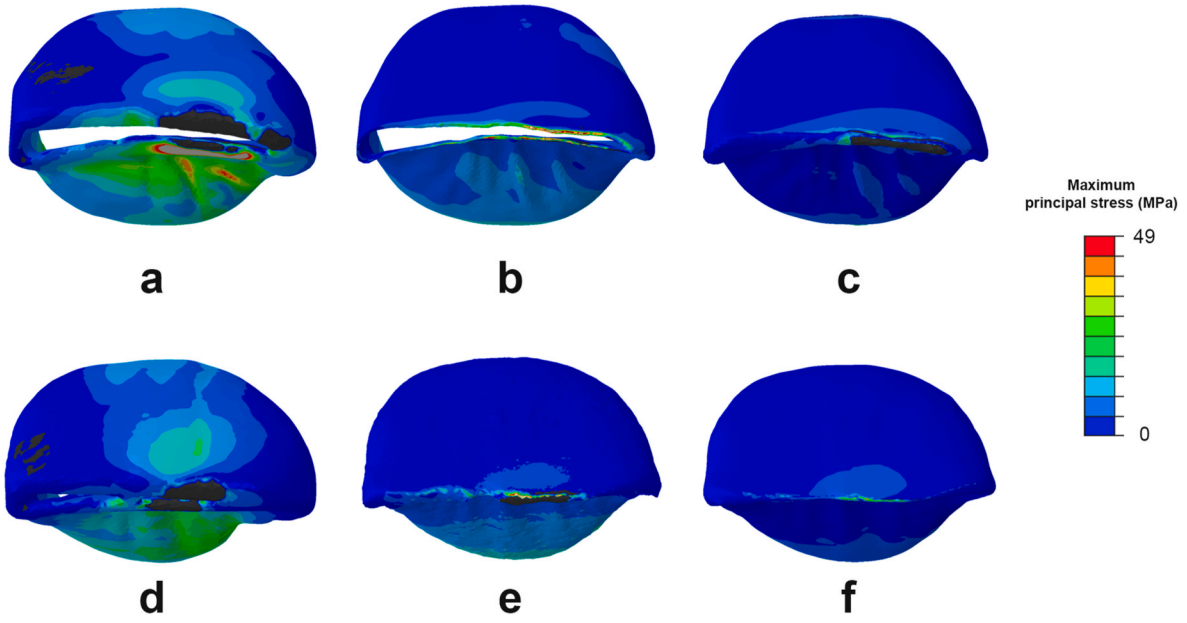

Fig. 7. Maximum principal stress distribution (MPa) of Le Moustier 1 (a, b, and c) and Qafzeh 9 (d, e, and f) left I^1 in occlusal view during edge-to-edge occlusion (applied force = 294.4 N). Enamel (a and d), enamel-dentine junction (b and e) and dentine (c and f).

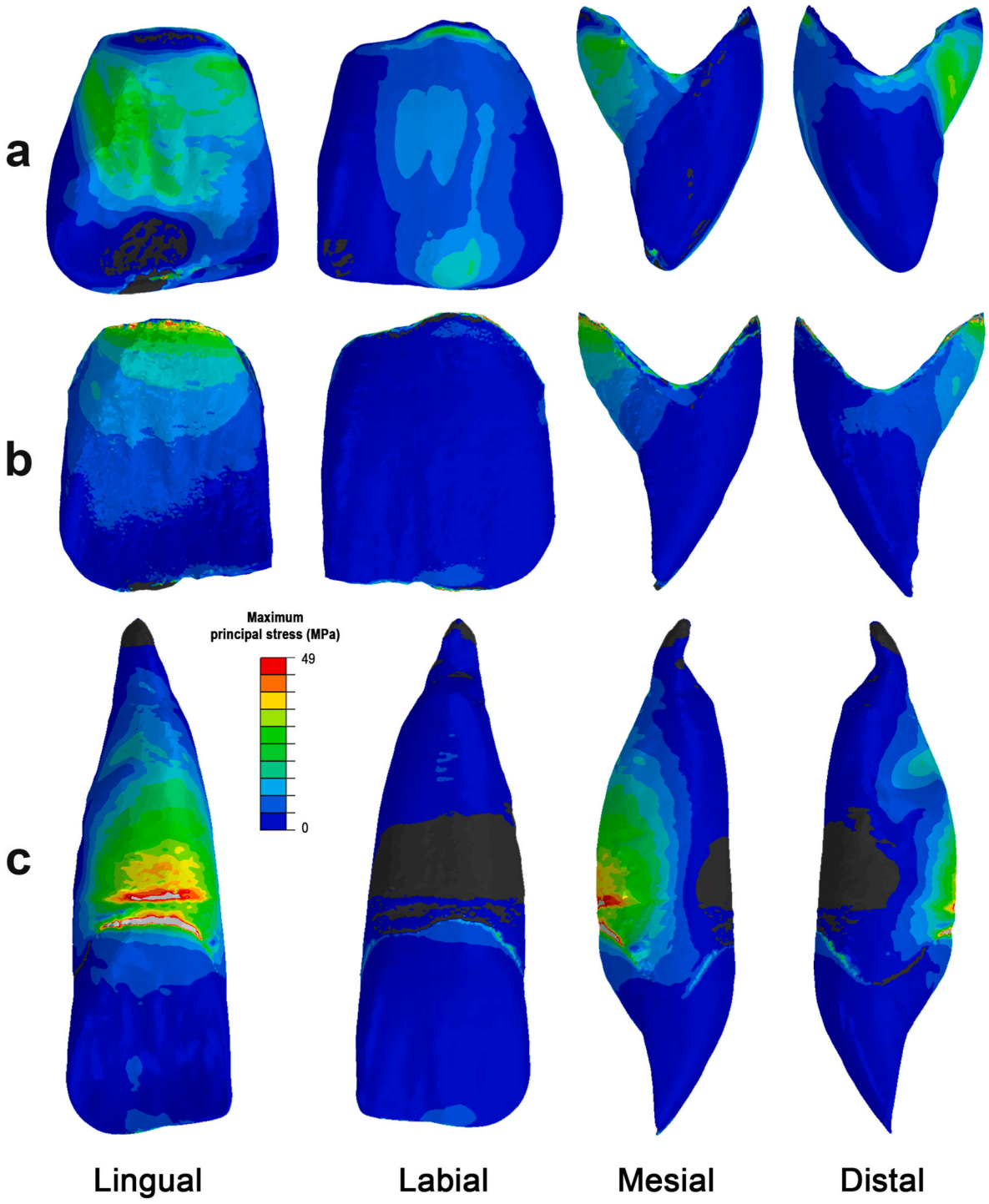

Fig. 9. Maximum principal stress distribution (MPa) of Qafzeh 9 1 left I^1 in lingual, labial, mesial and distal view during edge-to-edge occlusion (applied force = 188 N). Enamel (a), enamel dentine junction (b) and dentine (c).

9a; SOM Figs. S6b, S11a and S14g). We also observe moderate dotted areas of tensile stress along the labial surface, apical to the incisal load, in the middle and around the cervix. The EDJ shows only a few areas of tensile stress around the lingual aspect, especially along the cervical line (Figs. 7e and 9b; SOM Figs. S11a and S14h). In the crown, dentine does not show any tensile stress with the exception of a small area localized in correspondence of the incisal edge (Figs. 7e and 9b; SOM Figs. S11a and S14h).

Compressive stress in Qafzeh 9 left I^1 is mostly localized around the occlusal contact on the lingual aspect of the incisal edge and, to a lesser degree, on the labial surface (SOM Figs. S9b, S10b, S12a, S13a, S14a and S14d). Small areas of compressive stress can also be observed along the cervix, especially in its lingual and mesial aspect. Compressive stress is lower at EDJ level, with few areas of higher values located on the incisal edge (and on its labial and lingual aspect) and along the cervical line (SOM Figs. S9b, S10b, S12b, S13b, S14b and S14e). Finally, compressive stress of crown dentine is small and localized along the incisal edge (SOM Figs. S9b, S10b, S12c, S13c, S14c and S14f).

The root of Le Moustier 1 left I^1 shows high levels of tensile stress around the cervical and middle thirds (Figs. 6c and 8a; SOM Figs. S4c

and S6a), while compressive stress is mostly found on the labial aspect around the middle third, and below the cervical line, especially on its labial and distal aspects (SOM Figs. S7c, S8c, S9a and S10a). A similar tensile stress distribution is observed in the root of Qafzeh 9 I^1, with higher values located lingually around the cervical and middle thirds (Figs. 8b and 9c; SOM Figs. S6b and S11), while compressive stress is mostly found on the labial aspect around the middle thirds, and below the cervix (SOM Figs. S9b, S10b, S12c and S13c). A small area of moderate compressive stress is also found on the labial aspect of the apical region.

Finally, we also examined the orientation of maximum and minimum principal stress using vector plots. In Le Moustier 1 high maximum principal stress in enamel, EDJ and root dentine is mostly directed along the long axis of the tooth (SOM Figs. S15a–c). However, the tensile stress localized around the lingual grooves tends to be more oblique, and this is more evident at the EDJ level. Interestingly, the few dotted areas of moderate tensile stress in labial and in distal view run perpendicular to those observed in lingual and mesial view. The opposite situation is found with the orientation of minimum principal stress, where the tensile stress runs parallel to the long axis in labial and in distal view, while the same stress runs horizontally in lingual and mesial view (SOM Figs. S16a–c). In Qafzeh 9 left I^1 the orientation of tensile stress at the enamel and EDJ levels (in lingual and mesial view) is more oblique, but it becomes straighter and more parallel to the long axis of the tooth in the root region (SOM Figs. S17a–c). As observed in Le Moustier 1, tensile stress in labial and mesial view runs more horizontally. Minimum principal stress in Qafzeh 9 runs orthogonal to maximum principal stress (SOM Figs. S18a–c). The major difference between these two specimens is that the orientation of compressive stress in Qafzeh 9 is more localized. Furthermore, we observe a labial deformation along the incisal edge of the crowns of Le Moustier 1 and Qafzeh 9 (SOM Fig. 16a and 18a).

4. Discussion

The repositioning of Le Moustier 1 and Qafzeh 9 crowns allowed us to perform the kinematic occlusal simulation as realistic as possible, which was used to evaluate the mechanical behavior of discrete dental traits of maxillary incisors. In particular, in Le Moustier 1 we found that the lingual surface of the central maxillary incisor displays higher level of tensile stress under edge-to-edge loading conditions, while compressive stress is mostly localized on the labial side. Tensile stress is concentrated around the lingual fossa and in the cervical third, while compressive stress mostly develops around the occlusal contact areas and on the labial surface. On the contrary, Qafzeh 9 maxillary central incisor is characterized by a more homogenous and reduced distribution of tensile stress in the crown, especially in the enamel. However, the mesio-lingual aspects of its root display a more pronounced level of tensile stress around the cervical and middle thirds. Compressive stress in Qafzeh 9 left I^1 crown is reduced if compared to those observed in Le Moustier 1, especially on its labial surface. Moreover, we only found areas of compressive stress along its incisal edge at the enamel and the EDJ levels but not in dentine.

These initial results seem to indicate that the presence of well-developed labial convexity, strong lingual tubercle and moderate shoveling in Le Moustier maxillary incisor play an important role in dissipating mechanical loads during biting. It has been suggested that shoveled incisors in Inuit and in other human populations are of great importance for dissipating vertical occlusal forces, and they are considered to be part of the facial architecture associated with powerful biting forces (Hylander, 1977; Mizoguchi, 1985; Kanazawa et al., 2001; Pilbrow, 2006). These traits are also seen as byproducts of selection for other non-dental adaptations (Hlusko et al., 2018). Magne et al. (1999) found similar biomechanical results using recent modern human maxillary incisors when loaded on the incisal edge, showing that tensile stress develops along the palatal half of the tooth, while compressive stress is found in the facial half. These authors suggested that the presence of marginal ridges and cingulum contribute to decrease the level of stress on the lingual aspect of the crown. The results of our study quantitatively support Le Cabec et al. (2013) hypothesis which suggests that the presence of a pronounced lingual tubercle in Neanderthal incisors may represent a better adaptation to decrease the amount of stress generated from heavy or frequent loads on the labial portion of the anterior teeth.

If we have a closer look at the stress distribution of Le Moustier 1 central maxillary incisor under edge-to-edge occlusion we can notice that tensile stress is mostly concentrated along the grooves and fissures of the lingual fossa, and it concentrates near the cervix. Similar stress distribution results have been found in molars and premolars of modern humans, Neanderthals and great apes (Benazzi et al., 2011a, 2013a, 2013c, 2014b, 2015; Fiorenza et al., 2015). Probably high levels of tensile stresses along fissures and grooves of the tooth crowns help in reducing the general stress in the tooth elsewhere (Benazzi et al., 2011a). This is particularly evident in the sharp cusped molars of gorillas (Benazzi et al., 2013c) and in the crenulated surfaces of orangutan posterior teeth, which represent an adaptation to a diet of relative high hardness (Fiorenza et al., 2015). It is therefore possible to assume that the presence of grooves and fissures in the lingual fossa of maxillary incisors can help in better distributing the tensile stress to prevent tooth fracture, especially in unworn and slightly worn teeth (Benazzi et al., 2013a).

High tensile stresses around the cervical margins could be due to the weaker bond between enamel and dentine at the cervix and also because this area is characterized by thinner enamel (Goel et al., 1991; Benazzi et al., 2011a). Similar results have been found in premolars and molars of modern humans during maximum intercuspation loadings (Palamara et al., 2000; Chowdhary et al., 2008; Benazzi et al., 2011a). Interestingly, we found concentrated areas of tensile stress just above the cervical line in the mesial and distal aspect of the crown. This could be related to the lateral component of the bite force, which is one of the main forces responsible for the formation of interproximal wear (Wolpoff, 1971; Kaidonis et al., 1992; Benazzi et al., 2011a; Fiorenza et al., 2023). It has been suggested that differences in interproximal wear in human populations depend on diet and on food preparation methods (Hinton, 1982; Corruccini, 1990; Benazzi et al., 2011b). It is therefore possible that heavy occlusal loadings related to teeth-as-tool uses for daily-task activities could promote the formation of interproximal wear facets in the anterior dentition of Le Moustier 1. Benazzi et al. (2011a) showed that changes in forces distribution during occlusion in lower molars might explain the creation of interproximal wear facets. However, our simulation does not include the pressure from adjacent teeth. In fact, the second main component that promotes the formation of interproximal wear is the action of the mesial drift that causes the migration of teeth by bone remodeling and dental resorption (Moss and Picton, 1970; Sarig et al., 2016; Pokhojaev et al., 2018). Consequently, for a better understanding of this complex mechanism it will be necessary to carry out kinematic simulations that consider also the neighboring teeth (Benazzi et al., 2011a).

Qafzeh 9 left I^1 displays a more homogenous stress distribution, that in enamel is mostly found on the lingual aspect of the crown, without reaching high level of tensile stress that has been observed in Le Moustier 1.

It is possible that the reduction of tensile stress found in Qafzeh 9 is caused by its thicker enamel. In fact, Neanderthal teeth are characterized by a relatively thinner enamel than in modern humans (Olejniczak et al., 2008; Smith et al., 2012). The dental size reduction occurred in *H. sapiens* has caused a marked decrease of coronal dentine leading to relatively thicker enameled teeth in recent modern humans (Olejniczak et al., 2008; Smith et al., 2012). It is therefore possible that the presence of bulging incisors with relatively thinner enamel coupled with larger volume of coronal dentine in Neanderthals, may have increased tensile stresses in the enamel, ultimately requiring the development of some

compensatory features such as lingual tubercles and marginal ridges.

Le Moustier 1 left I^1 shows a 2D RET value which is significantly smaller compared to the average 2D values observed in other Neanderthals and in fossil and recent *Homo sapiens*. This could explain the absence of a strong shoveling, a feature typically observed in Neanderthal anterior teeth (Bailey, 2006, 2007). Qafzeh 9 left I^1 display also a significantly larger 2D and 3D RET values than those of Le Moustier 1, further confirming that the presence of thicker enamel helps to reduce the tensile stress in the crown. However, our study was limited to only two specimens. Consequently, to test this hypothesis we will need a larger sample size, including Neanderthal and modern humans characterized by accessory dental traits with variable degree of expression.

The underlying dentine of Le Moustier 1 and Qafzeh 9 maxillary incisor crowns do not show any sign of tensile stress labially and lingually. It seems that the EDJ absorbs most of the stress, confirming the results of previous studies that suggest that this intermediate tissue plays an important role to decrease tensile stress in the crown (Zaslansky et al., 2006; Shimizu and Macho, 2007; Zaytsev and Panfilov, 2014; Benazzi et al., 2015; Fiorenza et al., 2015). In fact, the presence of several layers having different properties can improve the resilience of interfaces (Suresh, 2001). That said, the microanatomy of EDJ is still poorly understood, and future investigations are needed to properly understand the mechanical behavior of this dental tissue. The only exception is the penetration of compressive stress in correspondence of the contact area with the lower teeth, especially in Le Moustier 1. It therefore appears that EDJ is not equally capable in reducing compressive stress in the underlying dentine, at least in Le Moustier 1. However, further studies are needed to investigate this mechanical behavior.

Neanderthals anterior roots are larger, longer and characterized by a different shape compared to those of modern humans (Le Cabec et al., 2012, 2013). Because teeth with greater root length or larger surface area resist better to high magnitude forces than teeth with short roots and with a small surface area (Schatz et al., 2011), Le Cabec et al. (2013) suggested that Neanderthal anterior root morphology could be an adaptation to better sustain high or frequent loads on the front teeth. Our initial results confirm this hypothesis. In fact, we found that the larger root surface of Le Moustier 1 left I^1 better resists to the applied force during edge-to-edge occlusion if compared to Qafzeh 9 maxillary central incisor, which is characterized by a smaller tooth surface and by a slender root shape.

Previous studies found greater root surface area on the labial side of the Neanderthal maxillary and mandibular incisors, suggesting that this is the side of the root where most tension occurs (Kloehn, 1938; Le Cabec et al., 2013). However, our FEA results show that in both Le Moustier 1 and Qafzeh 9 specimens the tensile stress is mostly distributed on the lingual aspect of the root and not on the labial side. This has been also observed in previous biomechanical studies showing that higher tensile stress can be found on the lingual aspect of the dental root (Magne et al., 1999; Benazzi et al., 2011a, 2014b). Massé et al. (2023) further suggested that greater cementum at the root apex is found in the lingual area. Therefore, it is possible that the greater labial convexity combined with marked angle between the crown and the root of Neanderthal incisors change the pattern of distribution of stress (Harris et al., 1993; Le Cabec et al., 2013). Hylander (1977) proposed that greater root surface area should be found in zone under high compressive force as a result of larger amount of periodontal fibers. Thus, the greater root surface area found labially could be an adaptive response to compressive rather than tensile stress, as seen in Le Moustier 1. However, it is important to note that stress distribution may differ in other biting scenarios. Dynamic FEA simulations (Benazzi et al., 2016) have shown that differences in loading directions affect the stress distribution in the tooth crowns. Consequently, while we did not observe high tensile stress on the labial aspect of the root during edge-to-edge occlusion, this may be not the case under different loading regimes. Future studies may address this question.

Interestingly, Le Cabec et al. (2013) have also observed a high degree of hypercementosis around the apical third of the Neanderthal incisor roots, which could represent another possible adaptation to sustain high or frequent occlusal loads on the anterior teeth. Some researchers have suggested that hypercementosis could influence the stress distribution since it alters the natural shape of the root (Le Cabec et al., 2013; García-González et al., 2019; Massé et al., 2023). The FEA results of Le Moustier 1 and Qafzeh 9 show higher compressive stress on the lingual surface of the root's apex, which agrees with Le Cabec et al. (2013) hypothesis that the excessive secretion cementum around the apical root third could represent a mechanical adaptation to resist repeated and frequent compression.

Although the main goal of our study was to test the functional adaptive hypothesis, other scholars have suggested that dental traits such as shoveling, lingual tuberculum or labial convexity are not adaptive but the by-product of neutral evolution (Kimura et al., 2009; Hlusko et al., 2018). Although the testing of these alternative hypotheses goes beyond the goal of this study, our preliminary results suggest that the presence/absence of these traits in maxillary central incisors lead to different mechanical stress distributions.

Finally, it is important to highlight some limitations of our FEA. First, although the detailed functional repositioning of Le Moustier 1 and Qafzeh 9 teeth and sophisticated digital approach consented us to investigate the mechanical behavior of incisor accessory traits in these two individuals, a larger sample size is needed to test if the morphology of Neanderthal anterior teeth represents an adaptation to sustain high mechanical load as suggested by the ADLH. Furthermore, incisor morphology in Neanderthals and in *Homo sapiens* is extremely variable (Le Cabec et al., 2013). In this context, our analysis should be considered only as preliminary. Future studies should include also modern human samples with known diets and known cultural habits to compare and evaluate the functional and mechanical behavior of accessory dental traits.

It is also important to note that Le Moustier 1 is adolescent individual whose dentition shows a normal bite position (Ponce de León and Zollikofer, 1999), and not the typical edge-to-edge occlusion which is expected to occur in an advanced adult ontogenetic stage, ubiquitous among the dentition of Neanderthals and other prehistoric humans (Kaifu et al., 2003). Moreover, Qafzeh 9 is characterized by an anterior-cross bite caused by a malposition of the left lateral incisor, which would have led to a posterior cross-bite during edge-to-edge occlusion (Sarig et al., 2013a). Although the anterior-cross bite in Qafzeh 9 does not affect the occlusal contact of the maxillary central incisor during edge-to-edge occlusion, it creates a locking mechanism during maximum intercuspation, preventing this tooth to occlude with its antagonist lower teeth (Sarig et al., 2013a). It is also possible that this type of malocclusion observed in Qafzeh 9 may have reduced the masticatory forces along the dental arch (Sarig et al., 2013b). However, this latter aspect needs further investigations. Furthermore, Qafzeh 9 root's apex was partially broken, and our virtual reconstruction may have not accurately captured its shape, which now looks like a pipette. Previous FE studies have shown that in teeth with a bent or pipette-shaped root significant tensile stress was concentrated at the root apex (Oyama et al., 2007). However, Qafzeh 9's root is not affected by tensile stress at the apex. Moreover, the compressive stress distribution at the root's apex it is very similar to those observed in Le Moustier 1. However, in the future we should test if using different virtual reconstruction of Qafzeh 9 root can lead to different FE results.

It should be also considered that due to the impacted lower canine and the presence of the deciduous canine in the arch in Le Moustier 1, the smaller mesio-distal dimension of the canine results in a shorter arch length that might also be the cause the lack of a natural edge-to edge occlusion. Edge-to-edge occlusion in the adults is the byproduct of extensive tooth wear accompanied by lingual tipping of the anterior teeth (Kaifu et al., 2003). Thus, Le Moustier 1 shows an intermediate condition that would eventually have led to a natural edge-to-edge occlusion (Ponce de León and Zollikofer, 1999). Consequently, Le Moustier

1 may not represent the best Neanderthal individual to test the ADLH. However, Le Moustier 1 is characterized by moderately worn anterior teeth, relative to the post-canine dentition, thus suggesting that this individual was already using incisors and canines as tools. The finite element comparison of the Le Moustier 1 teeth with those of adult Neanderthals can provide important insights on how mechanical stress changes during the ontogenetic transition from a normal to an edge-to-edge occlusion.

Second, we simplified our finite element models of Le Moustier 1 and Qafzeh 9 central maxillary incisors by attributing isotropic property to the enamel and dentine. However, enamel and dentine should be considered anisotropic because physical properties vary depending on the directions and regions of the tooth crown (Spencer and Demes, 1993; Lertchirakarn et al., 2001). Third, our simulations were based on static occlusion, and therefore they may not accurately reflect the functional responses of hard and soft tissues of a tooth. A recent study has shown that non-linear dynamic finite element crash colliding test represent more realistic simulation of the relationship between chewing behavior, tooth wear and occlusal loadings (Benazzi et al., 2016). Solving equations of non-linear finite element problems requires long processing time and very powerful computer. It would be however interesting to analyze how mechanical stress changes depending on the occlusal position, and when the anterior dentition is under maximum stress. Finally, our simulation only includes the interaction between upper and lower teeth. However, for a more accurate analysis of the ADLH, these simulations should also include various external objects (and with different material properties) embedded between the anterior teeth to examine the effect on the stress distribution over the teeth (Benazzi et al., 2015). The objects in between the teeth could be pulled in different directions to explore how stress is distributed during para-masticatory activities (Benazzi et al., 2015). However, the interactions between three objects in FEA is extremely complicated, and, at the moment, we are still not able to run these types of simulations.

5. Conclusions

In this study we provided a very detailed functional dental restoration of Le Moustier 1 and Qafzeh 9 human fossil specimens using a dental articulator and occlusal fingerprint analysis. We verified the occlusal positioning of the reconstructed dental arches carrying out a kinematic simulation via the OFA software (Kullmer et al., 2013). This has allowed us to identify the occlusal contact areas in Le Moustier 1 and Qafzeh 9 anterior teeth, which we used to load the maxillary central incisors for the finite element analysis. We found that the stress distribution in the enamel and in the root of Le Moustier 1 and Qafzeh 9 maxillary central incisors differs, probably in response to dental and root morphological differences and to enamel thickness variation. The results of our biomechanical test also suggest that during occlusion the tensile stress in enamel is distributed lingually, while compressive stress develop labially. Our results also confirm that EDJ represents an important intermediate tissue that helps in absorbing tensile stress. Most of the tensile stress in the root is found labially in correspondence of the cervical and middle third, while compressive stress develops labially and around the root's apex. Consequently, it seems that the combination of the lingual tubercle, labial convexity, moderate shoveling and large root surface in Le Moustier 1 contributed to dissipating compressive and tensile stresses. However, future studies are needed to test if these traits represent a biomechanical adaptation to sustain high or frequent occlusal load as suggested by the ADLH.

CRediT authorship contribution statement

Ali Najafzadeh: Writing – review & editing, Writing – original draft, Visualization, Validation, Software, Methodology, Investigation, Formal analysis. **María Hernaiz-García:** Writing – review & editing, Writing – original draft, Visualization, Investigation, Formal analysis, Data curation. **Stefano Benazzi:** Writing – review & editing, Writing – original draft, Visualization, Resources, Formal analysis, Data curation, Conceptualization. **Bernard Chen:** Writing – review & editing. **Jean-Jacques Hublin:** Writing – review & editing, Resources, Data curation. **Ottmar Kullmer:** Writing – review & editing, Writing – original draft, Visualization, Validation, Software, Resources, Methodology, Investigation, Formal analysis, Data curation. **Ariel Pokhojaev:** Writing – review & editing, Resources, Data curation. **Rachel Sarig:** Writing – review & editing, Resources, Data curation. **Rita Sorrentino:** Writing – review & editing, Writing – original draft, Visualization, Formal analysis, Data curation. **Antonino Vazzana:** Writing – review & editing, Writing – original draft, Visualization, Methodology, Formal analysis, Data curation. **Luca Fiorenza:** Writing – review & editing, Writing – original draft, Visualization, Supervision, Software, Project administration, Methodology, Investigation, Funding acquisition, Formal analysis, Data curation, Conceptualization.

Declaration of competing interest

There are no conflicts of interest.

Acknowledgments

We would like to thank Almud Hoffmann, the curator of the Museum für Vor-und Frühgeschichte in Berlin, for providing access to the original specimen and allowing the acquisition of μCT data of Le Moustier 1 bone remains. We are very thankful to Dieter Schulz, who has performed the professional physical and physiological repositioning of the dental crowns from high resolution casts. We also want to thank Christine Hemm for surface scanning the reconstructions of the dental arches of Le Moustier 1 and Qafzeh 9, and for preparing the single crown models for the kinematic OFA analysis. We also want to express our gratitude to Jana Storsberg, who did the detail OFA mapping of the macrowear facet pattern with the Polyworks Modeller module. Moreover, we are deeply indebted to Huynh Nguyen for his invaluable comments and suggestions on the creation of the finite element models. This study was supported by the Australian Research Council, Australia (grant number: DP190100465).

Supplementary Online Material

Supplementary Online Material to this article can be found online at https://doi.org/10.1016/j.jhevol.2024.103512.

References

Anton, S.C., 1994. Mechanical and other perspectives on Neandertal craniofacial morphology. In: Corruccini, R.S., Ciochon, R.L. (Eds.), Integrative Pathways to the Past: Paleoanthropological Advances in Honor of F. Clark Howell. Prentice Hall, New Jersey, pp. 677–695.

Bailey, S.E., 2006. Beyond shovel-shaped incisors: Neandertal dental morphology in a comparative context. Period. Biol. 108, 253–267.

Bailey, S.E., 2007. The Neandertal adolescent Le Moustier 1: New aspects, new results. J. Hum. Evol. 52, 227–229.

Bakke, M., 2006. Bite force and occlusion. Semin. Orthod. 12, 120–126.

Benazzi, S., Kullmer, O., Grosse, I.R., Weber, G.W., 2011a. Using occlusal wear information and finite element analysis to investigate stress distribution in human molars. J. Anat. 219, 259–272.

Benazzi, S., Fiorenza, L., Katina, S., Bruner, E., Kullmer, O., 2011b. Quantitative assessment of interproximal wear facet outlines for the association of isolated molars. Am. J. Phys. Anthropol. 144, 309–316.

Benazzi, S., Nguyen, H.N., Schulz, D., Grosse, I.R., Gruppioni, G., Hublin, J.-J., Kullmer, O., 2013a. The evolutionary paradox of tooth wear: Simply destruction or inevitable adaptation? PLoS One 8, e62263.

Benazzi, S., Kullmer, O., Schulz, D., Gruppioni, G., Weber, G.W., 2013b. Individual tooth wear pattern guides the reconstruction of Sts 52 (*Australopithecus africanus*) dental arches. Am. J. Phys. Anthropol. 150, 324–329.

Benazzi, S., Nguyen, H.N., Kullmer, O., Hublin, J.-J., 2013c. Unravelling the functional biomechanics of dental features and tooth wear. PLoS One 8, e69990.

Benazzi, S., Panetta, D., Fornai, C., Toussaint, M., Gruppioni, G., Hublin, J.-J., 2014a. Guidelines for the digital computation of 2D and 3D enamel thickness in hominoid teeth. Am. J. Phys. Anthropol. 153, 305–313.

Benazzi, S., Grosse, I.R., Gruppioni, G., Weber, G.W., Kullmer, O., 2014b. Comparison of occlusal loading conditions in a lower second premolar using three-dimensional finite element analysis. Clin. Oral Invest. 18, 369–375.
Benazzi, S., Nguyen, H.N., Kullmer, O., Hublin, J.-J., 2015. Exploring the biomechanics of taurodontism. J. Anat. 226, 180–188.
Benazzi, S., Nguyen, H.N., Kullmer, O., Kupczik, K., 2016. Dynamic modeling of tooth deformation using occlusal kinematics and finite element analysis. PLoS One 11, e0152663.
Brace, C.L., 1964. The fate of the "classic" Neanderthals: A consideration of hominid catastrophism. Curr. Anthropol. 5, 3–43.
Brace, C.L., 1967. Environment, tooth form, and size in the Pleistocene. J. Dent. Res. 46, 809–816.
Brůžek, J., Vandermeersch, B., 1997. Reassessment of the sex of the Qafzeh 9 individual based on multivariate statistical analysis. Am. J. Phys. Anthropol. Suppl. 24, 84.
Buti, L., Le Cabec, A., Panetta, D., Tripodi, M., Salvadori, P.A., Hublin, J.-J., Feeney, R.N. M., Benazzi, S., 2017. 3D enamel thickness in Neandertal and modern human permanent canines. J. Hum. Evol. 113, 162–172.
Cartagena, A.G., Sequeros, G., Garcia, V.C.C., 1996. Analysis of two methods for occlusal contact registration with the T-Scan system. J. Oral Rehabil. 24, 426–432.
Chowdhary, R., Lekha, K., Patil, N.P., 2008. Two-dimensional finite element analysis of stresses developed in the supporting tissues under complete dentures using teeth with different cusp angulations. Gerodontology 25, 155–161.
Clement, A.F., Hillson, S.W., Aiello, L.C., 2012. Tooth wear, Neanderthal facial morphology and the anterior dental loading hypothesis. J. Hum. Evol. 62, 367–376.
Coqueugniot, H.L., Tillier, A.M., Bruzek, J., 2000. Mandibular ramus posterior flexure: A sex indicator in *Homo sapiens* fossil hominids? Int. J. Osteoarchaeol. 10, 426–431.
Corruccini, R.S., 1990. Australian aboriginal tooth succession, interproximal attrition, and Begg's theory. Am. J. Orthod. Dentofac. Orthop. 97, 349–357.
Crameri, F., 2020. Scientific Colour Maps. http://www.fabiocrameri.ch/colourmaps.
Crameri, F., Shephard, G.E., Heron, P.J., 2020. The misuse of colour in science communication. Nat. Commun. 11, 5444.
Daumas, M., Chapman, T., Louryan, S., 2021. Le Moustier 1 Neandertal – the discovery of two new sets of casts, 3D reconstruction and comparison with original fossils. Digit. Appl. Archaeol. Cult. Heritage 23, e00204.
Demes, B., 1987. Another look at an old face: Biomechanics of the Neandertal facial skeleton reconsidered. J. Hum. Evol. 16, 297–303.
Dieck, W., 1923. Das Gebiß des diluvialen *Homo mousteriensis* Hauseri und seine Rekonstruktion. Odontol. Tidskr. 31, 196–209.
Eng, C.M., Lieberman, D.E., Zink, K.D., Peters, M.A., 2013. Bite force and occlusal stress production in hominin evolution. Am. J. Phys. Anthropol. 151, 544–557.
Fiorenza, L., Kullmer, O., 2013. Dental wear and cultural behaviour in Middle Paleolithic humans from the Near East. Am. J. Phys. Anthropol. 152, 107–117.
Fiorenza, L., Kullmer, O., 2015. Dental wear patterns in early modern humans from Skhul and Qafzeh: a response to Sarig and Tillier. HOMO 66, 414–419.
Fiorenza, L., Nguyen, H.N., Benazzi, S., 2015. Stress distribution and molar macrowear in *Pongo pygmaeus*: A new approach through finite element and occlusal fingerprint analyses. Hum. Evol. 30, 215–226.
Fiorenza, L., Benazzi, S., Kullmer, O., Zampirolo, G., Mazurier, A., Zanolli, C., Macchiarelli, R., 2019. Dental microwear and cortical bone distribution of the Neanderthal mandible from Regourdou (Dordogne, southwestern France). J. Hum. Evol. 132, 174–188.
Fiorenza, L., Benazzi, S., Estalrrich, A., Kullmer, O., 2020. Diet and cultural diversity in Neanderthals and modern humans from dental macrowear analyses. In: Schmidt, C., Watson, J.T. (Eds.), Dental Wear in Evolutionary and Biocultural Contexts. Academic Press, London, pp. 39–72.
Fiorenza, L., Habashi, W., Moggi-Cecchi, J., Benazzi, S., Sarig, R., 2023. Relationship between interproximal and occlusal wear in *Australopithecus africanus* and Neanderthal molars. J. Hum. Evol. 183, 103423.
Fu, G., Deng, F., Wang, L., Ren, A., 2010. The three-dimension finite element analysis of stress in posterior tooth residual root restored with postcore crown. Dent. Traumatol. 26, 64–69.
García-González, R., Sánchez-Puente, Z., Rodríguez, L., Quam, R.M., Carretero, J.M., 2019. Hypercementosis of the magdalenian human mandibular teeth from El Mirón cave, Cantabria (Spain). Quat. Int. 515, 150–158.
Goel, V.K., Khera, S.C., Ralston, J.L., Chang, K.H., 1991. Stresses at the dentinoenamel junction of human teeth – a finite element investigation. J. Prosthet. Dent 66, 451–459.
Harris, E.F., Hassankiadeh, S., Harris, J.T., 1993. Maxillary incisor crown-root relationships in different angle malocclusions. Am. J. Orthod. Dentofac. 103, 48e53.
Harrower, M., Brewer, C.A., 2003. ColorBrewer.org: an online tool for selecting colour schemes for maps. Cartographic J 40, 27–37.
Hillson, S., 2003. Dental Anthropology. Cambridge University Press, Cambridge.
Hinton, R.J., 1982. Differences in interproximal and occlusal tooth wear among prehistoric Tennessee Indians: Implications for masticatory function. Am. J. Phys. Anthropol. 57, 103–115.
Hlusko, L.J., Carlson, J.P., Chaplin, G., Elias, S.A., Hoffecker, J.F., Huffman, M., Jablonski, N.G., Monson, T.A., O'Rourke, D.H., Pilloud, M.A., Scott, G.R., 2018. Environmental selection during the last Ice Age on the mother-to-infant transmission of vitamin D and fatty acids through breast milk. Proc. Natl. Acad. Sci. USA 115, E4426–E4432.
Hoffmann, A., 1997. Zur Geschichte des Fundes von Le Moustier. Acta Praehist. Archaeol. 29, 7–16.
Hohmann, A., Kober, C., Young, P., Dorow, C., Geiger, M., Boryor, A., Sander, F.M., Sander, C., Sander, F.G., 2011. Influence of different modeling strategies for the periodontal ligament on finite element simulation results. Am. J. Orthod. Dentofacial Orthop. 139, 775–783.
Hylander, W.L., 1977. The adaptive significance of Eskimo craniofacial morphology. In: Dahlberg, A.A., Graber, T.M. (Eds.), Orofacial Growth and Development. Mouton Publishers, The Hague, pp. 129–169.
Kaidonis, J.A., Townsend, G.C., Richards, L.C., 1992. Brief Communication: Interproximal tooth wear: A new observation. Am. J. Phys. Anthropol. 88, 105–107.
Kaifu, Y., Kasai, K., Townsend, G.C., Richards, L.C., 2003. Tooth wear and the "design" of the human dentition: A perspective from evolutionary medicine. Yearb. Phys. Anthropol. 46, 47–61.
Kanazawa, E., Shirono, Y., Nakayama, M., Yamada, H., Hanamura, H., Kondo, S., 2001. Distribution of tubercle-shaped incisors in South Pacific populations. Anthropol. Sci. 109, 225–238.
Kay, R.F., Hiiemae, K.M., 1974. Jaw movement and tooth use in recent and fossil primates. Am. J. Phys. Anthropol. 40, 227–256.
Kimura, R., Yamaguchi, T., Takeda, M., Kondo, O., Toma, T., Hanji, K., Hanihara, T., Matsukusa, H., Kawamura, S., Maki, K., Osawa, M., Ishida, H., Oota, H., 2009. A common variation in EDAR is a genetic determinant of shovel-shaped incisors. Am. J. Hum. Gen. 85, 528–535.
Klaatsch, H., 1909. Die Fortschritte der Lehre von der Neandertal-Rasse. Ergebnisse anatomischer Entwicklungsgeschichte 17, 431–462.
Klaatsch, H., Hauser, O., 1908. *Homo mousteriensis Hauseri*: Ein altdiluvialer Skelettfund im Departement Dordogne und seine Zugehörigkeit zum Neandertaltypus. Arch. Anthropol. 7, 287–297.
Kloehn, S.J., 1938. The significance of root form as determined by occlusal stress. Angle Orthod. 8, 213–230.
Kono, R.T., 2000. Molar enamel thickness and distribution patterns in extant great apes and humans: New insights based on a 3-dimensional whole crown perspective. Anthropol. Sci. 112, 121–146.
Krueger, K.L., Ungar, P.S., 2012. Anterior dental microwear texture analysis of Krapina Neandertals. Cent. Eur. J. Geosci. 4, 651–662.
Krueger, K.L., Ungar, P.S., Guatelli-Steinberg, D., Hublin, J.-J., Pérez-Pérez, A., Trinkaus, E., Willman, J.C., 2017. Anterior dental microwear textures show habitat-driven variability in Neandertal behaviour. J. Hum. Evol. 105, 13–23.
Kullmer, O., Benazzi, S., Fiorenza, L., Schulz, D., Bacso, S., Winzen, O., 2009. Technical Note: Occlusal fingerprint analysis: Quantification of tooth wear pattern. Am. J. Phys. Anthropol. 139, 600–605.
Kullmer, O., Schulz, D., Benazzi, S., 2012. An experimental approach to evaluate the correspondence between wear facet position and occlusal movements. Anat. Rec. 295, 846–852.
Kullmer, O., Benazzi, S., Schulz, D., Gunz, P., Kordos, L., Begun, D.R., 2013. Dental arch restoration using tooth macrowear patterns with application to *Rudapithecus hungaricus*, from the late Miocene of Rudabanya, Hungary. J. Hum. Evol. 64, 151–160.
Kullmer, O., Menz, U., Fiorenza, L., 2020. Occlusal Fingerprint Analysis (OFA) reveal dental occlusal behaviour in primate teeth. In: Martin, T., von Koenigswald, W. (Eds.), Mammalian Teeth: Form and Function. Dr. F. Pfeil., Munich, pp. 25–43.
Lautenschlager, S., 2021. True colours or red herrings?: Colour maps for finite element analysis in palaeontological studies to enhance interpretation and accessibility. R. Soc. Open Sci. 8, 211357.
Le Cabec, A., Kupczik, K., Gunz, P., Braga, J., Hublin, J.J., 2012. Long anterior mandibular tooth roots in Neanderthals are not the result of their large jaws. J. Hum. Evol. 63, 667e681.
Le Cabec, A., Gunz, P., Kupczik, K., Braga, J., Hublin, J.-J., 2013. Anterior tooth root morphology and size in Neanderthals: Taxonomic and functional implications. J. Hum. Evol. 64, 169–193.
Ledogar, J.A., Smith, A.L., Benazzi, S., Weber, G.W., Spencer, M.A., Carlson, K.B., McNulty, K.P., Dechow, P.C., Grosse, I.R., Ross, C.F., Richmond, B.G., Wright, B.W., Wang, Q., Byron, C., Carlson, K.J., de Ruiter, D.J., Berger, L.R., Tamvada, K., Pryor, L.C., Berthaume, M.A., Strait, D.S., 2016. Mechanical evidence that *Australopithecus sediba* was limited in its ability to eat hard foods. Nat. Commun. 7, 10596.
Lertchirakarn, V., Palamara, J.E.A., Messer, H.H., 2001. Anisotropy of tensile strength of root dentin. J. Dent. Res. 80, 453.
Lugli, F., Nava, A., Sorrentino, R., Vazzana, A., Bortolini, E., Oxilia, G., Silvestrini, S., Nannini, N., Bondioli, L., Fewlass, H., Talamo, S., Bard, E., Mancini, L., Müller, W., Romandini, M., Benazzi, S., 2022. Tracing the mobility of a Late Epigravettian (~ 13 ka) male infant from Grotte di Pradis (Northeastern Italian Prealps) at high-temporal resolution. Sci. Rep. 12, 8104.
Magne, P., Versluis, A., Douglas, W.H., 1999. Rationalization of incisor shape: Experimental-numerical analysis. J. Prosthet. Dent 81, 345–355.
Marshall Jr., G.W., Balooch, M., Gallagher, R.R., Gansky, S.A., Marshall, S.J., 2001. Mechanical properties of the dentinoenamel junction: AFM studies of nanohardness, elastic modulus, and fracture. J. Biomed. Mater. Res. 54, 87–95.
Martin, L., 1985. Significance of enamel thickness in hominoid evolution. Nature 314, 260–263.
Martinón-Torres, M., Bermúdez de Castro, J.M., Gómez-Robles, A., Arsuaga, J.L., Carbonell, E., Lordkipanidze, D., Manzi, G., Margvelashvili, A., 2007. Dental evidence on the hominin dispersals during the Pleistocene. Proc. Natl. Acad. Sci. USA 104, 13279–13282.
Martinón-Torres, M., Bermúdez de Castro, J.M., Gómez-Robles, Prado-Simón, L., Arsuaga, J.L., 2012. Morphological description and comparison of the dental remains from Atapuerca-Sima de los Huesos site (Spain). J. Hum. Evol. 62, 7–58.
Massé, L., Garot, E., Maureille, B., Le Cabec, A., 2023. Insights into the aetiologies of hypercementosis: A systematic review and a scoring system. Arch. Oral Biol. 146, 105599.
Maureille, B., Turq, A., 2005. Le Moustier sites' excavations and their importance in French archaeology. In: Ullrich, H. (Ed.), The Neanderthal Adolescent Le Moustier 1,

New Aspects, New Results. StaatlicheMuseen zu Berlin, Preußischer Kulturbesiz, Berlin, pp. 21–28.
Mellars, P., Grün, R., 1991. A comparison of the electron spin resonance and thermoluminescence dating methods: The results of ESR dating at Le Moustier (France). Camb. Archaeol. J. 1, 269–276.
Mizoguchi, Y., 1985. Shovelling: A Statistical Analysis of its Morphology. Tokyo University Press, Tokyo.
Molnar, S., 1972. Tooth wear and culture: A survey of tooth functions among some prehistoric populations. Curr. Anthropol. 13, 511–526.
Moss, J.P., Picton, D.C.A., 1970. Mesial drift of teeth in adult monkeys (*Macaca irus*) when forces from the cheeks and tongue had been eliminated. Arch. Oral Biol. 15, 979–986.
Nicholson, E., Harvati, K., 2006. Quantitative analysis of human mandibular shape using three-dimensional geometric morphometrics. Am. J. Phys. Anthropol. 131, 368–383.
Nogueira, D.C., Dutour, O., Coqueugniot, H., Tillier, A.-m., 2019. Qafzeh 9 mandible (ca 90-100 kyrs BP, Israel) revisited: μ-CT and 3D reveal new pathological conditions. Int. J. Paleopath. 26, 104–110.
Olejniczak, A.J., Smith, T.M., Feeney, R.N.M., Macchiarelli, R., Mazurier, A., Bondioli, L., Rosas, A., Fortea, J., de la Rasilla, M., Garcia-Tabernero, A., Radovčić, J., Skinner, M. M., Toussaint, M., Hublin, J.J., 2008. Dental tissue proportions and enamel thickness in Neandertal and modern human molars. J. Hum. Evol. 55, 12–23.
Oyama, K., Motoyoshi, M., Hirabayashi, M., Hosoi, K., Shimizu, N., 2007. Effects of root morphology on stress distribution at the root apex. Eur. J. Orthod. 29, 113–117.
O'Connor, C.F., Franciscus, R.G., Holton, N.E., 2005. Bite force production capability and efficiency in Neandertals and modern humans. Am. J. Phys. Anthropol. 127, 129–151.
O'Hara, M.C., Guatelli-Steinberg, D., 2022. Reconstructing tooth crown heights and enamel caps: A comparative test of three existing methods with recommendations for their use. Anat. Rec. 305, 123–143.
Palamara, D., Palamara, J.E.A., Tyas, M.J., Messer, H.H., 2000. Strain patterns in cervical enamel of teeth subjected to occlusal loading. Dent. Mater. 16, 412–419.
Panagiotopoulou, O., 2009. Finite element analysis (FEA): Applying an engineering method to functional morphology in anthropology and human biology. Ann. Hum. Biol. 36, 609–623.
Pilbrow, V., 2006. Lingual incisor traits in modern hominoids and assessment of their utility for fossil hominoid taxonomy. Am. J. Phys. Anthropol. 129, 323–338.
Pokhojaev, A., Habashi, W., May, H., Schulz-Kornas, E., Shvalb, N., Sarig, R., 2018. Examination of the interproximal wear mechanism: facet morphology and surface texture analysis. J. Dent. Res. 13, 1445–1451.
Ponce de León, M.S., 2002. Computerized palaeoanthropology and Neanderthals: The case of Le Moustier 1. Evol. Anthropol. 11, 68–72.
Ponce de León, M.S., Zollikofer, C.E., 1999. New evidence from Le Moustier 1: Computer-assisted reconstruction and morphometry of the skull. Anat. Rec. 254, 474–489.
Puech, P.F., 1981. Tooth wear in La Ferrassie man. Curr. Anthropol. 22, 424–430.
Rak, Y., 1986. The Neanderthal: A new look at an old face. J. Hum. Evol. 15, 151-1.
Rayfield, E.J., 2007. Finite element analysis and understanding the biomechanics and evolution of living and fossil organisms. Annu. Rev. Earth Planet Sci. 35, 541–576.
Sarig, R., Slon, V., Abbas, J., May, H., Shpack, N., Vardimon, A.D., Hershkovitz, I., 2013a. Malocclusion in early anatomically modern human: a reflection on the etiology of modern dental misalignment. PLoS One 8, e80771.
Sarig, R., Lianopoulos, N.V., Hershkovitz, I., Vardimon, A.D., 2013b. The arrangement of the interproximal interface in the human permanent dentition. Clin. Oral Investig. 17, 731–738.
Sarig, R., Gopher, A., Barkai, R., Rosell, J., Blasco, R., Weber, G.W., Fornai, C., Sella-Tunis, T., Hershkovitz, I., 2016. How did the Qesem Cave people use their teeth? Analysis of dental wear patterns. Quat. Int. 398, 136–147.
Schatz, D., Alfter, G., Göz, G., 2001. Fracture resistance of human incisors and premolars: Morphological and patho-anatomical factors. Dent. Traumatol. 17, 167–173.
Schuchardt, C., 1912. Die neue Zusammensetzung des Schädels von *Homo mousteriensis hauseri*. Amtl. Ber. aus den Königl. Kunstsammlungen, Beil. z. Jahrb. d. Königl. Preuss. Kunstsammlungen 34, 4–10.
Schwarcz, H., Grün, R., Vandermeersch, B., Bar-Yosef, O., Valladas, H., Tchernov, E., 1988. ESR dates for the hominid burial site of Qafzeh in Israel. J. Hum. Evol. 17, 733–737.
Scott, G.R., Turner II, C.G., 1997. The Anthropology of Modern Human Teeth. In: Dental Morphology and its Variation in Recent Human Populations. Cambridge University Press, Cambridge.
Shimizu, D., Macho, G.A., 2007. Functional significance of the microstructural detail of the primate dentino-enamel junction: A possible example of exaptation. J. Hum. Evol. 52, 103–111.
Smith, F.H., Paquette, S.P., 1989. The adaptive basis of Neandertal facial form, with some thoughts on the nature of modern human origins. In: Trinkaus, E. (Ed.), The Emergence of Modern Humans. Cambridge University Press, Cambridge, pp. 181–210.
Smith, H.B., 1984. Patterns of molar wear in hunter-gatherers and agriculturalists. Am. J. Phys. Anthropol. 63, 39–56.
Smith, T.M., Olejniczak, A.J., Zermeno, J.P., Tafforeau, P., Skinner, M.M., Hoffmann, A., Radovčić, J., Toussaint, M., Kruszynski, R., Menter, C., Moggi-Cecchi, J., Glasmacher, U.A., Kullmer, O., Schrenk, F., Stringer, C., Hublin, J.-J., 2012. Variation in enamel thickness within the genus *Homo*. J. Hum. Evol. 62, 395–411.
Spencer, M.A., Demes, B., 1993. Biomechanical analysis of masticatory system configuration in Neandertals and Inuits. Am. J. Phys. Anthropol. 91, 1–20.
Strait, D.S., Constantino, P., Lucas, P.W., Richmond, B.G., Spencer, M.A., Dechow, P.C., Ross, C.F., Grosse, I.R., Wright, B.W., Wood, B.A., Weber, G.W., Wang, Q., Byron, C., Slice, D.E., Chalk, J., Smith, A.L., Smith, L.C., Wood, S., Berthaume, M., Benazzi, S., Dzialo, C., Tamvada, K., Ledogar, J.A., 2013. Viewpoints. Diet and dietary adaptations in early hominin: The hard food perspective. Am. J. Phys. Anthropol. 151, 339–355.
Suresh, S., 2001. Graded materials for resistance to contact deformation and damage. Science 292, 2447–2451.
Thompson, J.L., Illerhaus, B., 1998. A new reconstruction of the Le Moustier 1 skull and investigation of internal structures using 3-D-μCT data. J. Hum. Evol. 35, 647–665.
Tillier, A.-M., Duday, H., Arensburg, B., Vandermeersch, B., 2004. Dental pathology, stressful events, and disease in Levantine early anatomically modern humans: Evidence from Qafzeh. In: Goren-Inbar, N., Speth, J.D. (Eds.), Human Paleoecology in the Levantine Corridor. Oxbow Books, Oxford, pp. 135–148.
Trinkaus, E., 1983. The Shanidar Neandertals. Academic Press, New York.
Trinkaus, E., 1986. The Neandertals and modern human origins. Annu. Rev. Anthropol. 15, 193–218.
Trinkaus, E., 1987. The Neandertal face: Evolutionary and functional perspectives on a recent hominid face. J. Hum. Evol. 16, 429–443.
Trinkaus, E., 1992. Morphological contrasts between the Near Eastern Qafzeh-Skhul and late archaic human samples: Grounds for behavioural difference? In: Akazawa, T., Aoki, K., Kimura, T. (Eds.), The Evolution and Dispersal of Modern Humans in Asia. Hokusen-Sha, Tokyo, pp. 277–294.
Turner II, C.G., Nichol, C.R., Scott, G.R., 1991. Scoring procedures for key morphological traits of the permanent dentition: The Arizona State University Dental Anthropology System. In: Kelley, M.A., Larsen, C.S. (Eds.), Advances in Dental Anthropology. Wiley-Liss, New York, pp. 13–31.
Ungar, P.S., Fennell, K.J., Gordon, K., Trinkaus, E., 1997. Neandertal incisor beveling. J. Hum. Evol. 32, 407–421.
Valladas, H., Geneste, J.M., Joron, J.L., Chadelle, J.P., 1986. Thermoluminescence dating of Le Moustier (Dordogne, France). Nature 322, 452–454.
Valladas, H., Reyss, J.L., Joron, J.L., Valladas, G., Bar Yosef, O., Vandermeersch, B., 1988. Thermoluminescence dating of Mousterian "Proto-cro-magnon" remains from Israel and the origin of modern Man. Nature 331, 614–616.
Van der Walt, S., Smith, N., 2015. A Better Default Colormap for Matplotlib. SciPy, 2015.
Vandermeersch, B., 1981. Les Hommes Fossiles de Qafzeh. CNRS Editions, Paris.
Vandermeersch, B., Bar-Yosef, O., 2019. The paleolithic burials at Qafzeh cave, Israel. PALEO 30, 256–275.
Wallace, J.A., 1975. Did La Ferrassie I use his teeth as a tool? Curr. Anthropol. 16, 393–401.
Weaver, T.D., 2009. The meaning of Neandertal skeletal morphology. Proc. Natl. Acad. Sci. USA 106, 16028–16033.
Weinert, H., 1925. Der Schädel des Eiszeitlichen Menschen von Le Moustier in Neuer Zusammensetzung. Springer, Berlin.
Wolpoff, M.H., 1971. Interstitial wear. Am. J. Phys. Anthropol. 34, 205–228.
Wroe, S., Ferrara, T.L., McHenry, C.R., Curnoe, D., Chamoli, U., 2010. The craniomandibular mechanics of being human. Proc. R. Soc. B 277, 3579–3586.
Wroe, S., Parr, W.C.H., Ledogar, J., Bourke, J., Evans, S.P., Fiorenza, L., Benazzi, S., Hublin, J.-J., Stringer, C., Kullmer, O., Curry, M., Rae, T.C., Yokley, T.R., 2018. Computer simulations show that Neanderthal facial morphology represents adaptation to cold and high energy demands, but not heavy biting. Proc. R. Soc. A B 285, 20180085.
Xia, Z., Jiang, F., Chen, J., 2013. Estimation of periodontal ligament's equivalent mechanical parameters for finite element modeling. Am. J. Orthod. Dentofacial Orthop. 143, 486–491.
Zaslansky, P., Friesem, A.A., Weiner, S., 2006. Structure and mechanical properties of the soft zone separating bulk dentin and enamel in crowns of human teeth: insight into tooth function. J. Struct. Biol. 153, 188–199.
Zaytsev, D., Panfilov, P., 2014. Deformation behaviour of human enamel and dentin-enamel junction under compression. Mater. Sci. Eng. 34, 15–21.